AD_____

Award Number: DAMD17-02-1-0714

TITLE: Evaluation and Refinement of a System and a Method for the Use of Hyperspectral Imaging for Metabolic Monitoring

PRINCIPAL INVESTIGATOR: James R. Mansfield

CONTRACTING ORGANIZATION: Hypermed, Incorporated
Watertown, MA 02472

REPORT DATE: September 2003

TYPE OF REPORT: Final

PREPARED FOR: U.S. Army Medical Research and Materiel Command
Fort Detrick, Maryland 21702-5012

REPORT DOCUMENTATION PAGE

Form Approved OMB No. 074-0188

1. AGENCY USE ONLY (Leave blank)	2. REPORT DATE	3. REPORT TYPE AND DATES COVERED
	September 2003	Final (1 Oct 2002 - 30 Sep 2003)

4. TITLE AND SUBTITLE

Evaluation and Refinement of a System and a Method for the Use of Hyperspectral Imaging for Metabolic Monitoring

5. FUNDING NUMBERS

DAMD17-02-1-0714

6. AUTHOR(S)

James R. Mansfield

7. PERFORMING ORGANIZATION NAME(S) AND ADDRESS(ES)

HyperMed, Incorporated
Watertown, MA 02472

E-Mail: jmansfield@hypermed-inc.com

8. PERFORMING ORGANIZATION REPORT NUMBER

9. SPONSORING / MONITORING AGENCY NAME(S) AND ADDRESS(ES)

U.S. Army Medical Research and Materiel Command
Fort Detrick, Maryland 21702-5012

10. SPONSORING / MONITORING AGENCY REPORT NUMBER

11. SUPPLEMENTARY NOTES

Original contains color plates: ALL DTIC reproductions will be in black and white

12a. DISTRIBUTION / AVAILABILITY STATEMENT

Approved for Public Release; Distribution Unlimited

12b. DISTRIBUTION CODE

13. ABSTRACT (Maximum 200 Words)

The primary hypothesis was that the mean grayscale intensity of hyperspectral oxygen saturation images in a region of interest (ROI) will change during hemorrhagic shock and during hypothermia. Secondary endpoints included the qualitative appearance of the ROI in the HSI images, and a quantitative measure of tissue heterogeneity (including patterns of diffuse heterogeneity and mottling). The relationship of skin blood flow, of sympathetic nerve activity, and of catecholamine levels to these changes were also to be explored.

Using the HSIMM methodologies developed for this study, it was possible to clearly differentiate ($p << 0.01$) between control and bleed groups in a porcine hypovolemia model. A stable hypovolemia model and data processing methods were developed to enable the transition of the technology and methodology into routine use at the Institute of Surgical Research. A pilot hypothermia study was performed, and HSIMM parameters were found to vary both with core temperature and skin contact temperature during hypothermia.

14. SUBJECT TERMS

15. NUMBER OF PAGES
39

16. PRICE CODE

17. SECURITY CLASSIFICATION OF REPORT	18. SECURITY CLASSIFICATION OF THIS PAGE	19. SECURITY CLASSIFICATION OF ABSTRACT	20. LIMITATION OF ABSTRACT
Unclassified	Unclassified	Unclassified	Unlimited

Technologies for Metabolic Monitoring FY2002

Evaluation and Refinement of a System and a Method for the Use of Hyperspectral Imaging for Metabolic Monitoring

DAMD17-02-1-0714

James R. Mansfield, P.I.

Jenny E. Freeman, Co - PI

Leopoldo Cancio, Andriy Batchinsky, Svetlana Panasyuk, Robert A. Lew

Table of Contents

COVER PAGE 1

REPORT DOCUMENTATION PAGE 2

TABLE OF CONTENTS 4

TABLE OF FIGURES 5

INTRODUCTION 7

BACKGROUND 7
PROPOSED STUDY 7
HYPOTHESIS 7
SUMMARY 7

BODY 8

MATERIALS AND METHODS 8
Hyperspectral Imaging System Development *8*
Development of a Porcine Model of Hemorrhagic Shock *8*
Preliminary Imaging Results *9*
RESULTS FROM THE HEMORRHAGIC SHOCK STUDY 12
Qualitative Analyses *12*
Image Heterogeneity Analysis 13
Oxygen Saturation Timecourse Analysis 15
Total Hemoglobin Time Course Analysis 17
Statistical Analyses *19*
Overall Imaging Variable Analyses 19
Summary of Hypovolemia Results *20*
RESULTS FROM THE HYPOTHERMIA STUDY 21
Individual protocols *21*
Overall Results *22*
Hypothermia Summary *26*

KEY RESEARCH ACCOMPLISHMENTS 27

REPORTABLE OUTCOMES 27

PRESENTATIONS 27
PUBLICATIONS 28
NEW PROJECTS AND OTHER OUTCOMES 29

CONCLUSIONS 30

APPENDICES 31

A. PORCINE HYPOVOLEMIC SHOCK MODEL METHODS .....
Animals .....
Surgical Preparation .....

Experiment: Hemorrhage and Resuscitation
Experiment: Hypothermia
Assays
B. LASER DOPPLER IMAGING METHODS
C. HYPERSPECTRAL IMAGING METHODS
Camera System
Data Collection
HSI data processing
D. Statistical Analysis
Statistical analyses
Mean Values by Stage for All Animals and Separately for Each Type
Primary Endpoints and Imaging Parametersfor Stages 2-7
Metabolic-Physiological Parameters for Stages 2-7
REFERENCES 39

Table of Figures

Figure 1: HSI camera and lighting system used for all procedures. Quartz-halogen light is arranged parallel to imaging axis. 8
Table 1: Timings and Events of Hypovolemia Protocol 9
Figure 2: Imaging Region on Inner Hindlimb. Left panel shows an actual optical density (OD) image from one dataset. Right panel shows an overview photo of a different animal showing general imaging region. Fiducial marks are arranged in a 2.5" x 5" square. 10
Figure 3: Time series of spectra from inner hindlimb. White box in left panel indicates region from which spectra were taken. The blue spectrum (right panel) shows a greater contribution from the oxy-Hb doublet, while the black spectrum, taken during maximum shock, shows no oxy-Hb. 11
Figure 4: Representation of the 4-term least square fitting used to generate O_2Sat and THb values from each spectrum in the image cube. 11
Figure 5: Four selected timepoints from a single bleed animal showing heterogeneity and correlation of HSI changes with physiological measurements. 12
Figure 6: O_2sat images from bleed animals, showing a baseline image and an image during the nadir of shock. All animals showed a decrease in the mean grayscale value, and all animals showed at least some changes in the pattern of oxygenation, with some (such as animal 345) showing considerable changes. 14
Figure 6: O_2sat images from control animals during baseline and during endpoint. No animal showed any significant changes in either mean grayscale value or in the pattern of the oxygenation during the course of the protocol. 14
Figure 8: Left panel shows the time courses of the relative O_2sat of each animal, with control animals show in green and bleed animals shown in red. Right panel shows the same data, which has been baseline corrected by subtracting the mean of the baseline period (image cubes 1 through 6) from each timepoint. Key timepoints of interest: 0: begin bleed; 70: begin LR resuscitation; 120: begin blood resuscitation 15

Figure 9: Average trends of control and bleed group relative oxygen saturation. Average of bleed group is shown in red; average of control group is shown in blue. Note approximately linear decrease in skin O_2Sat during entire bleed period and its partial recovery following LR resuscitation. Full recovery happens during blood reinfusion, resulting in a slight hyperemia. Error bars (one standard deviation) are shown on alternate timepoints to enhance visibility. 16
Figure 10: Left panel shows the time courses of the relative total hemoglobin of each animal, with control animals shown in green and bleed animals shown in red. Right panel shows the same data which has been baseline corrected by subtracting the mean of the baseline period (image cubes 1 through 6) from each time point. Key time points of interest: 0: begin bleed; 70: begin LR resuscitation; 120: begin blood resuscitation 17
Figure 11: Average trends of relative total hemoglobin for control and bleed groups. Average of control animals is shown in blue; average of bleed animals is shown in red. Following LR resuscitation, the THb level of the bleed groups is significantly lower than the control animals, and then recovers almost to baseline following blood reinfusion. Error bars (one standard deviation) are shown on alternate timepoints for clarity. 18
Equation 1: Pathlength calculation 19
Figure 12: Shows the average (± one standard deviation) of the six imaging variables (oxy-Hb, deoxy-Hb, offset and slope coefficients and the O_2Sat and THb) for the bleed and control groups, with the control group on the left and the bleed group on the right. Also shows the results (p-value) for the t-tests on the pathlength calculations for each of the imaging variables. 20
Figure 13: Second animal's hypothermia results. Rectal temperature is shown in green; O_2Sat (upper panel) and THb (lower panel) are shown in blue. Note that the THb trend changes when the under-blanket cooling parameters were changed, which is before the internal temperature of the animal begins to respond. 22
Figure 14: The third animal's hypothermia results. Rectal temperature is shown in green; O_2Sat and THb are shown in blue. Note that again the THb trend changes when the under-blanket cooling parameters were changed, which is before the internal temperature of the animal begins to respond while the O_2Sat values hardly change. 23
Figure 15: The fourth animal's hypothermia results. Rectal temperature is shown in green; O_2Sat and THb are shown in blue. Note that again the THb trend changes when the under-blanket cooling parameters were changed, which is before the internal temperature of the animal begins to respond while the O_2Sat values hardly change. 24
Figure 16: The fifth animal's hypothermia results. Rectal temperature is shown in green; O_2Sat and THb are shown in blue. Note that again the THb trend changes when the under-blanket cooling parameters were changed, which is before the internal temperature of the animal begins to respond while the O_2Sat values hardly change. 25

Introduction

Background

There is a global need for improved methods of metabolic monitoring. Different applications include: healthy athlete-soldiers during physical exertion; astronauts during EVA, brittle diabetics experiencing diurnal and sporadic fluctuations in insulin and glucose levels; and injured patients with hemorrhagic shock. To be maximally useful, metabolic monitoring should be non-invasive and easy to use. In this protocol, we propose assessing the use of hyperspectral imaging (HSI), for remote non-invasive metabolic monitoring. By examining the local tissue, HSIMM (Hyperspectral Imaging for Metabolic Monitoring) provides information about the physiology and metabolism of the organism of the whole. HSIMM takes advantage of the fact that the skin is readily available, providing a non-invasive "window" through which to view the metabolism. HSIMM can be useful in research designed to assess treatment protocols, pharmaceutical regimens or nutritional options. It can also be developed into a robust end-user device for the field or clinic. In this proposal, extreme physiologic states were studied by quantifying and depicting spatial changes in hemoglobin (Hb) oxygen saturation in the skin. Relating these local changes to systemic physiology will provide a generic understanding of the capabilities and limitations of HSIMM, and permit it to be generalized subsequently to other areas in which non-invasive metabolic monitoring would be highly advantageous.

Proposed Study

Based on our previous work, we believed that HSI could be used to monitor metabolism and pathophysiology. In order to explore broadly the applicability of this technology, we proposed to evaluate HSIMM of the skin during experiments designed to create two distinct alterations in systemic and cutaneous physiology: 1) hemorrhage and resuscitation and 2) hypothermia.

Hypothesis

The primary hypothesis was that the mean grayscale intensity of hyperspectral oxygen saturation images in a region of interest (ROI) will change during hemorrhagic shock and during hypothermia. Secondary endpoints included the qualitative appearance of the ROI in the HSI images, and a quantitative measure of tissue heterogeneity (including patterns of diffuse heterogeneity and mottling). The relationship of skin blood flow, of sympathetic nerve activity, and of catecholamine levels to these changes were also to be explored.

Summary

Using the HSIMM methodologies developed for this study, it was possible to clearly differentiate ($p << 0.01$) between control and bleed groups in a porcine hypovolemia model. A stable hypovolemia model and data processing methods were developed to enable the transition of the technology and methodology into routine use at the Institute of Surgical Research. A pilot hypothermia study was performed, and HSIMM parameters were found to vary both with core temperature and skin contact temperature during hypothermia.

Body

Materials and Methods

Hyperspectral Imaging System Development

The first stage of the project involved the development of a turnkey hyperspectral imaging (HSI) system which would integrate into the data collection scheme already in place at ISR. To this end, an existing CCD camera (Kodak MegaPLUS 1.6i) and visible wavelength liquid crystal tunable filter (LCTF) were incorporated into the system shown in Figure 1.

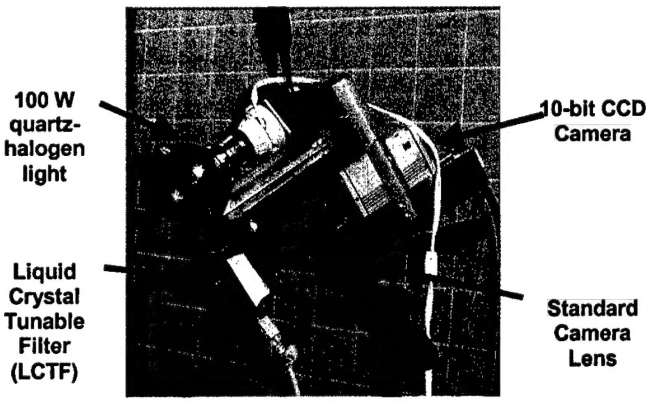

Figure 1: HSI camera and lighting system used for all procedures. Quartz-halogen light is arranged parallel to imaging axis.

A 100 W quartz-halogen light powered from a Sorenson 150 W DC power supply (Elgar Electronics, San Diego, CA) was incorporated and designed to provide co-axial illumination in the imaging axis of the camera system. Software was developed under the LabVIEW system (National Instruments Corporation, Austin, TX) to control the CCD camera and the LCTF, and to allow the data to be saved in an easily transportable binary format. All aspects of the image acquisition, such as number of images per wavelength to co-add and the binning factor for the camera CCD elements were controlled with the LabVIEW software. This software also allows easy integration of the HSI system data collection into the existing data acquisition (DAQ) system currently in use at ISR.

A complete description of the specific imaging parameters and equipment used in the experiments can be found in Appendix C.

Development of a Porcine Model of Hemorrhagic Shock

Prior to beginning the full controlled study, work needed to be done to develop a robust and repeatable hemorrhagic shock model with which to test our hypotheses. While hemorrhagic models have long been used in the study of shock and resuscitation, we needed to select and validate a model that would be reproducible and most useful for the collection and interpretation of HSIMM data. In addition to determining the answers to questions about the model itself, we also needed to answer specific questions about the acquisition of imaging data and how to best incorporate the two together.

Nine animals were used to develop the stable hemorrhagic shock model for this experiment, given an anesthesia regimen chosen to minimize skin effects and to be maximally reproducible. With an anesthesia regimen of isoflurane induction and ketamine maintenance, the first four animals were used to determine the volume of blood which must be withdrawn to ensure the animals would be in deep shock at the nadir, while allowing for no more than a 15% premature death rate. It was determined that 3 x 10 cc/kg bleeds was optimal. Three more animals were

used to determine the HSI protocol to be used, defining the body site, lighting requirements, the timing of image acquisition, data processing requirements, and the integration of the HSI data acquisition with the physiological data acquisition. The remaining animals were used to further refine the protocol, and to test out all of the parameters under the SOPs.

The final hypovolemia protocol followed the sequence of events shown in Table 1, with all times being given relative to the beginning of the first bleed at t = 0 min. HS images were acquired every 5 minutes unless otherwise specified.

Table 1: Timings and Events of Hypovolemia Protocol

Stage	Time (min)	Name	Events
1	-40 to –10	Baseline	Images 1 to 6 acquired
2	0 to 10	Bleed One	10 cc/kg bleed over 10 minutes. Images 7 and 8 acquired.
3	10 to 25	Recovery One	Images 9 and 10 acquired. PAWP and CO measured
4	25 to 35	Bleed Two	10 cc/kg bleed over 10 minutes. Images 11 and 12 acquired.
5	35 to 50	Recovery Two	Images 13 and 14 acquired. PAWP and CO measured
6	50 to 60	Bleed Three	10 cc/kg bleed over 10 minutes. Images 15 and 16 acquired.
7	60 to 75	Recovery Three	Images 17 and 18 acquired. PAWP and CO measured
8	75 to 100	LR Resuscitation	Images 19 to 23 acquired
9	100 to 130	Equilibration One	Images 24 to 29 acquired. PAWP and CO measured
10	130 to 155	Blood Resuscitation	Images 30 to 35 acquired
11	155 to 185	Equilibration Two	Images 36 to 42 acquired
12	185 to 215	Equilibration Three	Images 43 to 46 acquired. PAWP and CO measured.

Seventeen of twenty-three animals survived this protocol to the end. Control animals were treated identically to bleed animals, including undergoing a splenectomy and having all arterial and venous lines inserted, but had no blood removed and were not given any resuscitation fluid.

Preliminary Imaging Results

The inner hindlimb of the animal was chosen for several reasons. Firstly, a peripheral site was required to test the effects of shock on the peripheral blood flow. Secondly, the ventral surfaces of the animals are free of hair and blemishes. The size of the region imaged was chosen to maximize information relative to the spatial distribution of the mottling effects we were expecting to observe.

Figure 2 shows the final imaging area used for both the hemorrhagic shock and the hypothermia studies. The image on the left shows a 600 nm reflectance image taking using the HSI system

and shows the exact size and area of the animal being studies. The crosses are black ink fiducial marks drawn on the skin of the animal prior to the study for subsequent image registration and form a rectangle approximately 5 x 2.5 inches in size. The image on the right in Figure 2 shows a color photograph taken of an area slightly larger than that imaged by the HSI system, but which shows the inner hindlimb area more clearly.

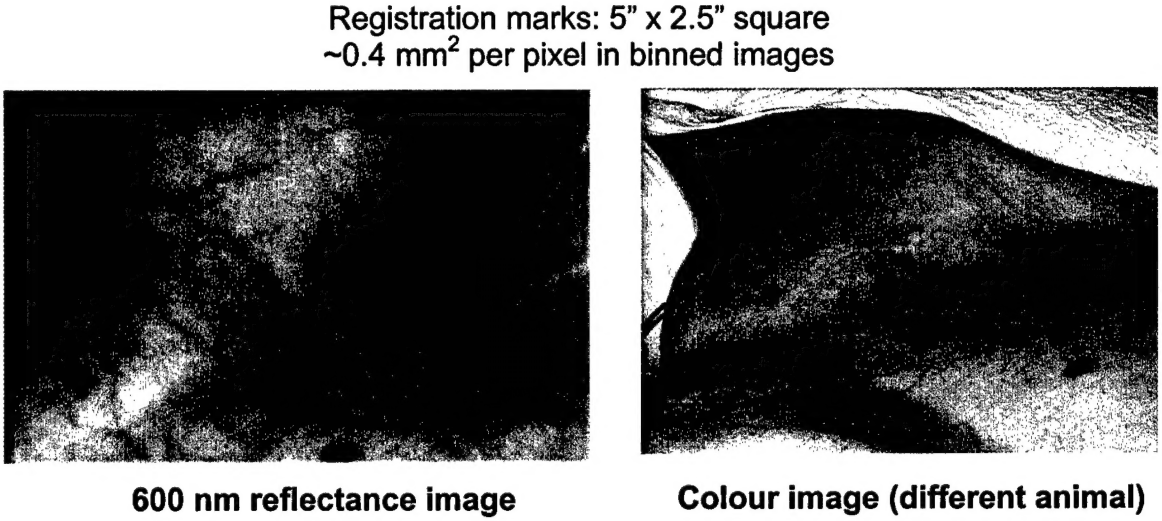

Figure 2: Imaging Region on Inner Hindlimb. Left panel shows an actual optical density (OD) image from one dataset. Right panel shows an overview photo of a different animal showing general imaging region. Fiducial marks are arranged in a 2.5" x 5" square.

Figure 3 shows the imaging region from one of the model development animals. The left image is an optical density image (see Appendix C for details on calculating optical density images). The right panel shows averaged spectra extracted from the region of the white box superimposed on the left panel. These spectra were obtained at various time points during the bleed phase of the study. The blue spectrum, taken during the initial baseline period, shows two peaks, indicating the presence of oxy-Hb. Following the third bleed, during the recovery period, the black spectrum shows no sign of oxy-Hb. This was confirmation that our imaging site would give useful data.

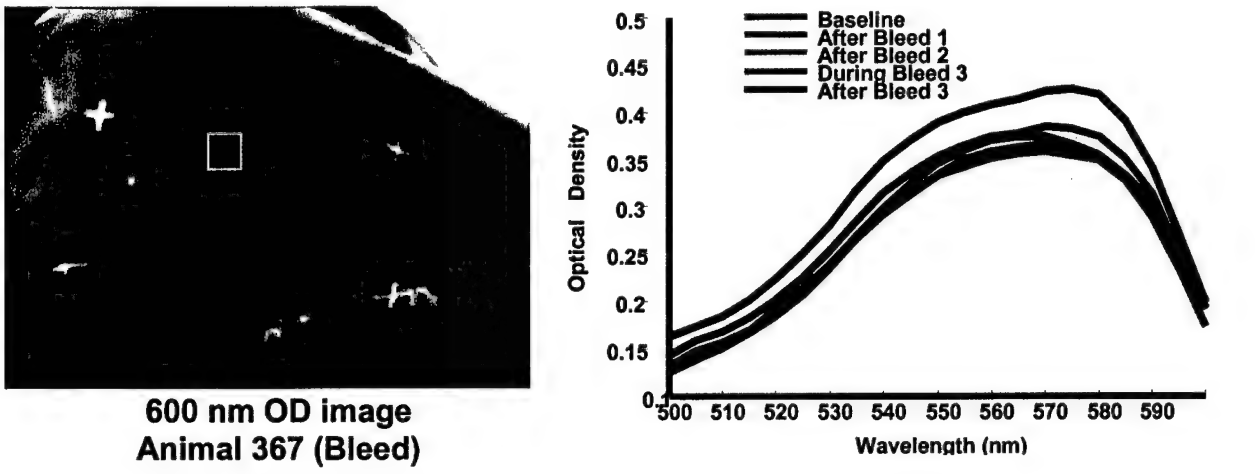

Figure 3: Time series of spectra from inner hindlimb. White box in left panel indicates region from which spectra were taken. The blue spectrum (right panel) shows a greater contribution from the oxy-Hb doublet, while the black spectrum, taken during maximum shock, shows no oxy-Hb.

In and of itself, data based on average changes in oxygenation provides useful information about tissue oxygenation and metabolism in the hindlimb during shock. The delivery of an average of 64,000 parallel spectra over a ROI is clearly superior to a point spectroscopic measurement (such as NIRS or TcPO2) in terms of minimizing sampling errors. However, to fully exploit the utility of HSIMM it is also important to determine the spatial heterogeneity in the oxygenation parameters across the imaged region. To this end, relative oxygen saturation and total hemoglobin images were calculated for each timepoint in each study.

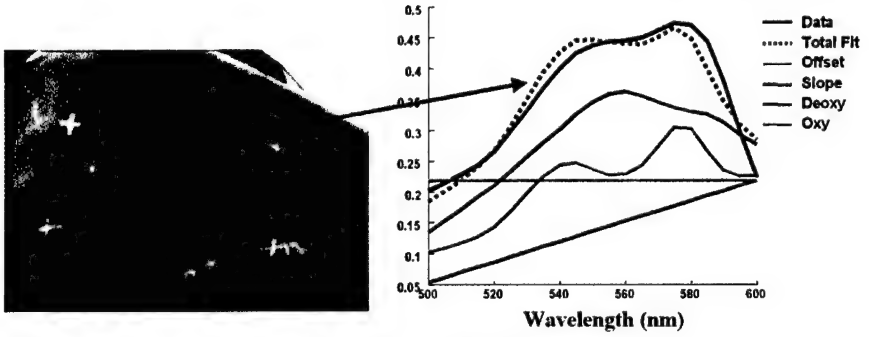

$$S_{ij} = \left\| c_{ij} Oxy + c_{ij} Deoxy + c_{ij} Offset + c_{ij} Slope \right\|_2$$

Figure 4: Representation of the 4-term least square fitting used to generate O_2Sat and THb values from each spectrum in the image cube.

Figure 4 (above) shows the four term least squares regression fitting of reference oxy-Hb, deoxy-Hb, an offset term and a slope term to each of the spectra of each image cube. From the fit coefficients, images of the relative oxygen saturation (O_2Sat) and total hemoglobin (THb) were calculated. Complete descriptions of the calculation of O_2Sat and THb images have been published elsewhere.[1,2]

Results from the Hemorrhagic Shock Study

Qualitative Analyses

Twenty-three animals were utilized in the full hemorrhagic shock study. Of those twenty-three animals, seventeen completed the entire shock procedure. The data from these seventeen animals were used in all of the results in this section, with no animals excluded or outlier determinations made.

Of the seventeen animals, 9 were bleed animals and 8 were control. This gave a sample size of 8 (df = 7) for all subsequent statistical calculations. O_2Sat and THb images were calculated for each of the approximately 46 time points in each of the 17 animals. In addition to obtaining full oxygenation images of the inner hindlimb, mean grayscale values from within an approximately 2 x 2 inch ROI on the flat surface of the inner hindlimb were calculated from each of the full images. These mean grayscale oxygen saturation values could then be compared on a timepoint by timepoint basis across both groups of animals (control and bleed). This gave a total of six HSI variables per timepoint: oxy-Hb; deoxy-Hb; offset; slope; O_2Sat and THb. The O_2Sat and THb values are calculated from the Oxy-Hb and deoxy-Hb fit coefficient variables and, as such, are not independent variables. However, as most of the information on skin oxygenation, both normally and during shock, is in terms of O_2Sat and THb, these variables were tested along with the four independent variables in order to facilitate interpretation of results.

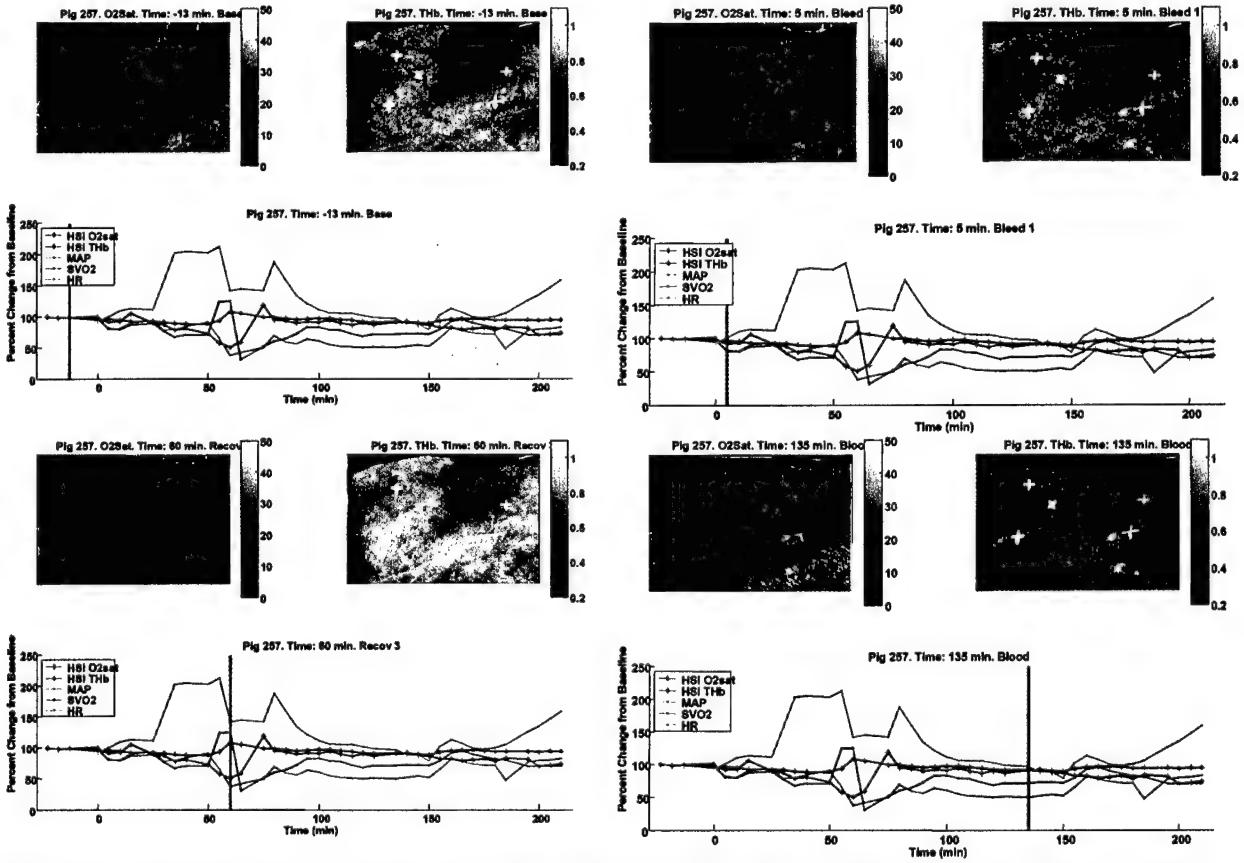

Figure 5: Four selected timepoints from a single bleed animal showing heterogeneity and correlation of HSI changes with physiological measurements.

The above images (Figure 5) demonstrate four selected time points in one of our studies. We have similar readings recorded at two minute intervals throughout the procedure. Note the slightly mottled appearance at baseline and very subtle pattern changes in the O_2Sat image at 5 minutes into the first bleed when the total O_2Sat reading was still nearly at baseline. The images on the bottom left represent data from 60 minutes into recovery after the last bleed and before the initiation of fluid resuscitation. The image at the bottom right follows resuscitation with both ringers lactate and blood and has returned to a mean value comparable to the baseline. Note, however that the pattern is quite different. This animal went on later to have an increasing heart rate and falling blood pressure before the end of the procedure and "did not look good" at the time it was euthanized. We could hypothesize that were the study protracted that it might not have survived.

In the particular animal shown in Figure 5 there was a profound heart rate rise which preceded the fall in blood pressure and SVO2. In the course of the 19 animals of the study, as has been often demonstrated we found no physiological parameters (heart rate, blood pressure, SVO2, MAP) that independently provided a consistent measure of the onset or depth of shock.

Image Heterogeneity Analysis

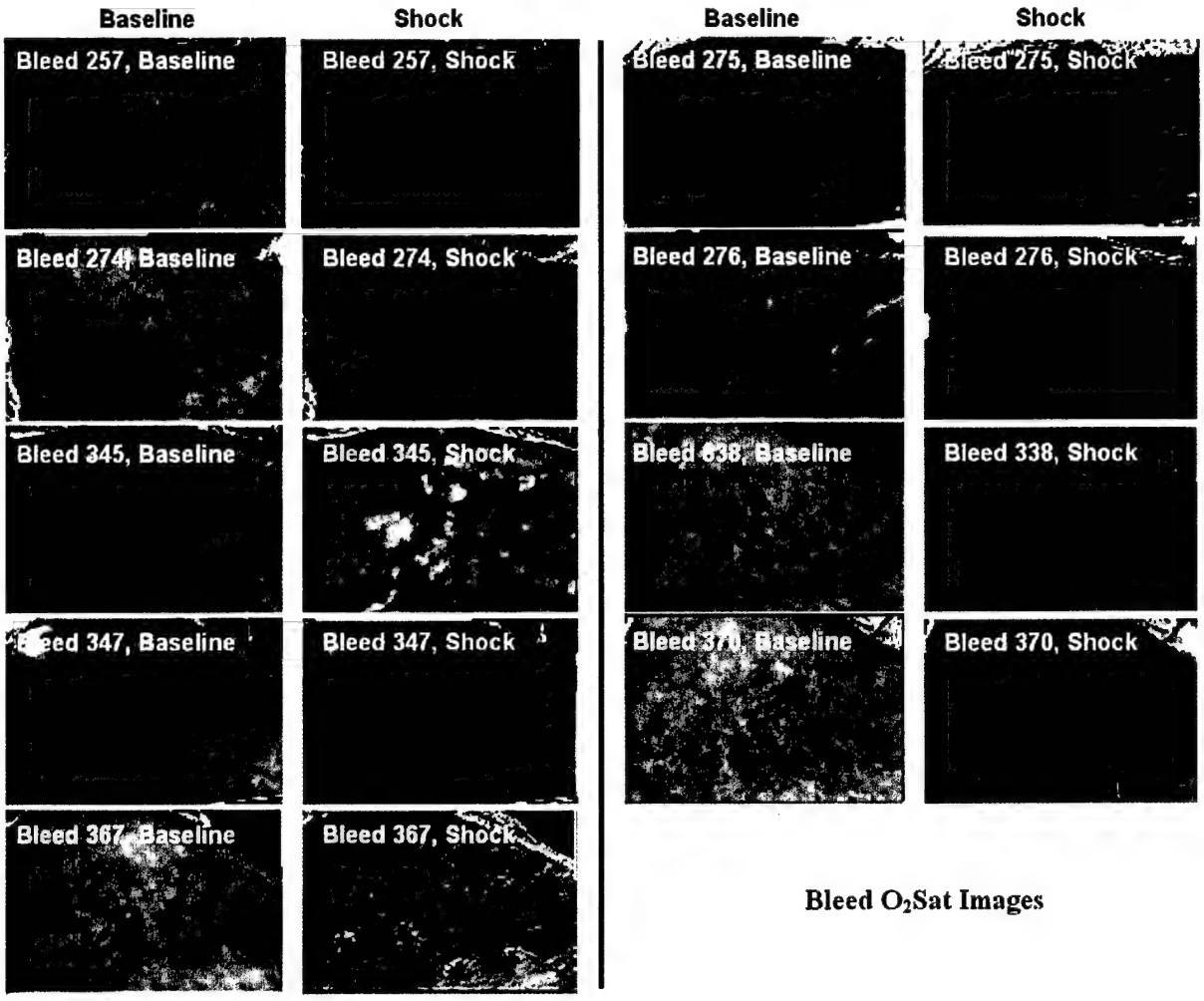

Bleed O_2Sat Images

Figure 6: O_2sat images from bleed animals, showing a baseline image and an image during the nadir of shock. All animals showed a decrease in the mean grayscale value, and all animals showed at least some changes in the pattern of oxygenation, with some (such as animal 345) showing considerable changes.

Figure 6 (above) shows O_2Sat images from the baseline period and from the nadir of shock for each of the bleed animals. Each animal has its own characteristic pattern of oxygenation (see for comparison the control animals in Figure 7 below), which remains relatively constant in this model until disturbed by the consequences of blood loss. Each bleed animal remained stable during its thirty-minute baseline period, following which both the mean grayscale value of the O_2Sat images and the pattern of oxygenation began to change.

At the nadir of shock, each of the bleed animals had undergone significant changes in both the mean grayscale values of the ROI and in the spatial heterogeneity pattern of oxygenation across the hindlimb. There were a variety of spatial heterogeneity responses seen in the eight bleed animals. Some, like animal 345, underwent significant mottling, with high and low oxygenation values approaching 100 and 0 percent O_2Sat, respectively. Others, like animal 370 exhibited little mottling, and showed only overall average grayscale changes. Other animals, such as 347 and 257, showed a new pattern, heretofore unseen, which we are terming "feathery" because of the characteristic pattern.

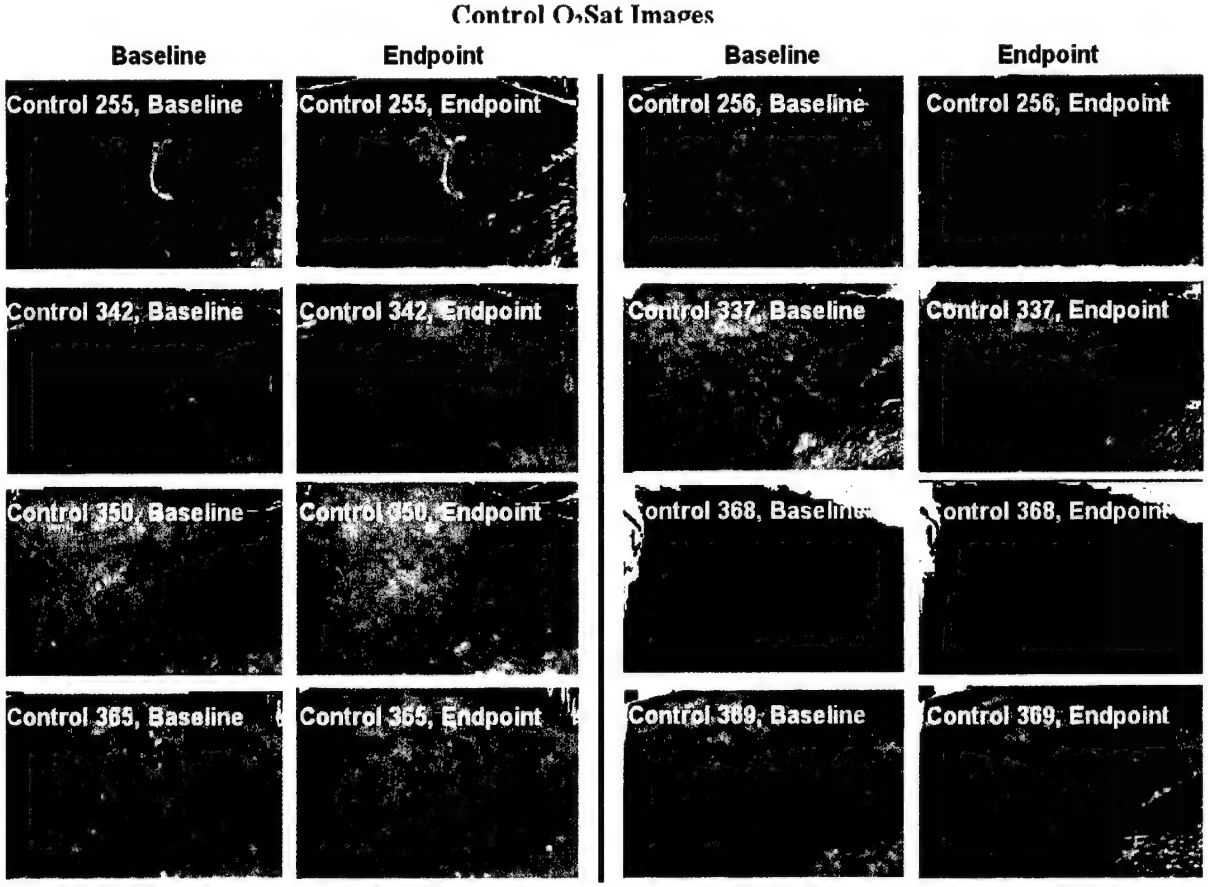

Figure 6: O_2sat images from control animals during baseline and during endpoint. No animal showed any significant changes in either mean grayscale value or in the pattern of the oxygenation during the course of the protocol.

Figure 7 (above) shows O_2Sat images from the baseline period and at the endpoint of the protocol for each of the control (sham bleed) animals. None of the animals showed any significant changes in either the mean grayscale value or the pattern of oxygenation during the course of the protocol. One animal (control 368) had an abnormally low but unchanging oxygenation level throughout the course of the protocol.

Overall, the bleed animals are clearly differentiable from the control animals in terms of both the mean grayscale values and the overall changes in spatial heterogeneity of the O_2Sat images.

However, in all cases, both for the bleed and for the control animals, no significant changes to the heterogeneity of the total hemoglobin (THb) images were seen. As is shown below, there were significant changes to the mean grayscale values of the THb images between the control and bleed groups, but no mottling patterns of any kind were observed for the THb images. This supports our concept that the mottling patterns observed in the O_2Sat images are related to oxygen extraction in the skin and not to the amount of blood there.

Oxygen Saturation Timecourse Analysis

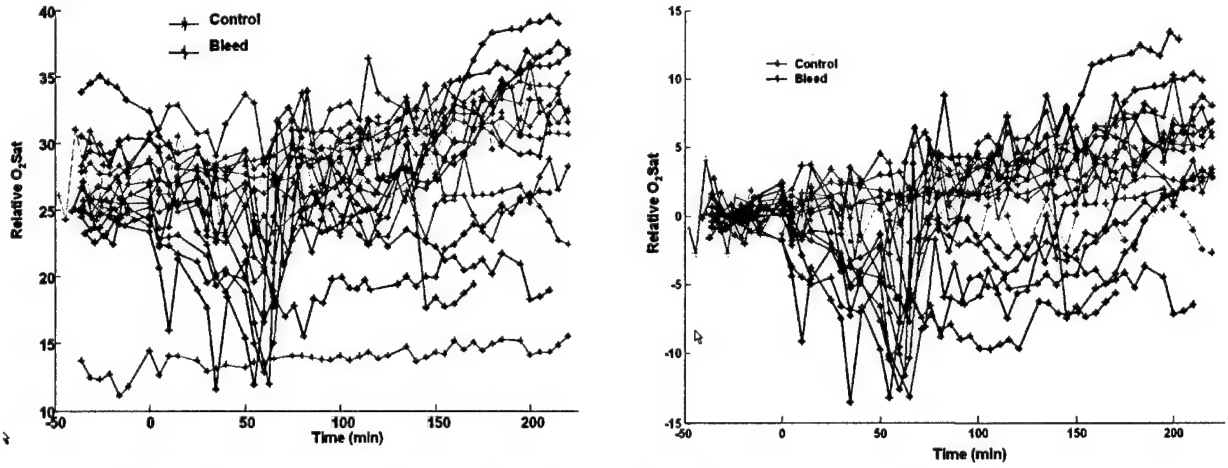

Figure 8: Left panel shows the time courses of the relative O_2sat of each animal, with control animals show in green and bleed animals shown in red. Right panel shows the same data, which has been baseline corrected by subtracting the mean of the baseline period (image cubes 1 through 6) from each timepoint. Key timepoints of interest: 0: begin bleed; 70: begin LR resuscitation; 120: begin blood resuscitation

Figure 8 (above) shows all of the time courses of the mean grayscale O_2Sat values extracted from the 2" x 2" ROI on the inner hindlimb. Control animals are shown in green while bleed animals are shown in red. The left panel shows the raw data while the right panel shows the baseline-subtracted data, where the mean value from the thirty-minute baseline period for each animal is subtracted from that time series.

As can be seen in both representations, the control animals exhibited very little change in the mean O_2Sat of the ROI during the 3.5 hours of the study, although this is more easily observed in the right panel. There is perhaps a slight increase in the mean O_2Sat of the ROI over time, which could represent a subtle response to the anesthesia and experimental environment.

The bleed animals, however, all showed a significant change in the mean O_2Sat values during the course of the study. All of the animals showed a decrease in O_2Sat during the bleed portion of the study (t = 0 to t = 75 min). Following resuscitation with lactated Ringer's (LR) solution at t = 75 min, most of the bleed animals showed an increase in their mean O_2sat values. However, as can be seen from the baseline corrected plots in the right panel of Figure 7, only a small number (n = 3) of the bleed animals returned to an O_2sat value corresponding to what the control animals had following LR resuscitation (t = 75 min). We consider the fact that all animals had a response to bleeding, but that there was significant variability relative to the characteristics of this response, to be very encouraging relative to the development of algorithms to predict adequacy of resuscitation or survivability.

Following blood resuscitation (t = 125 to t = 150 min), each of the bleed animals showed a further increase in O_2sat values within the ROI.

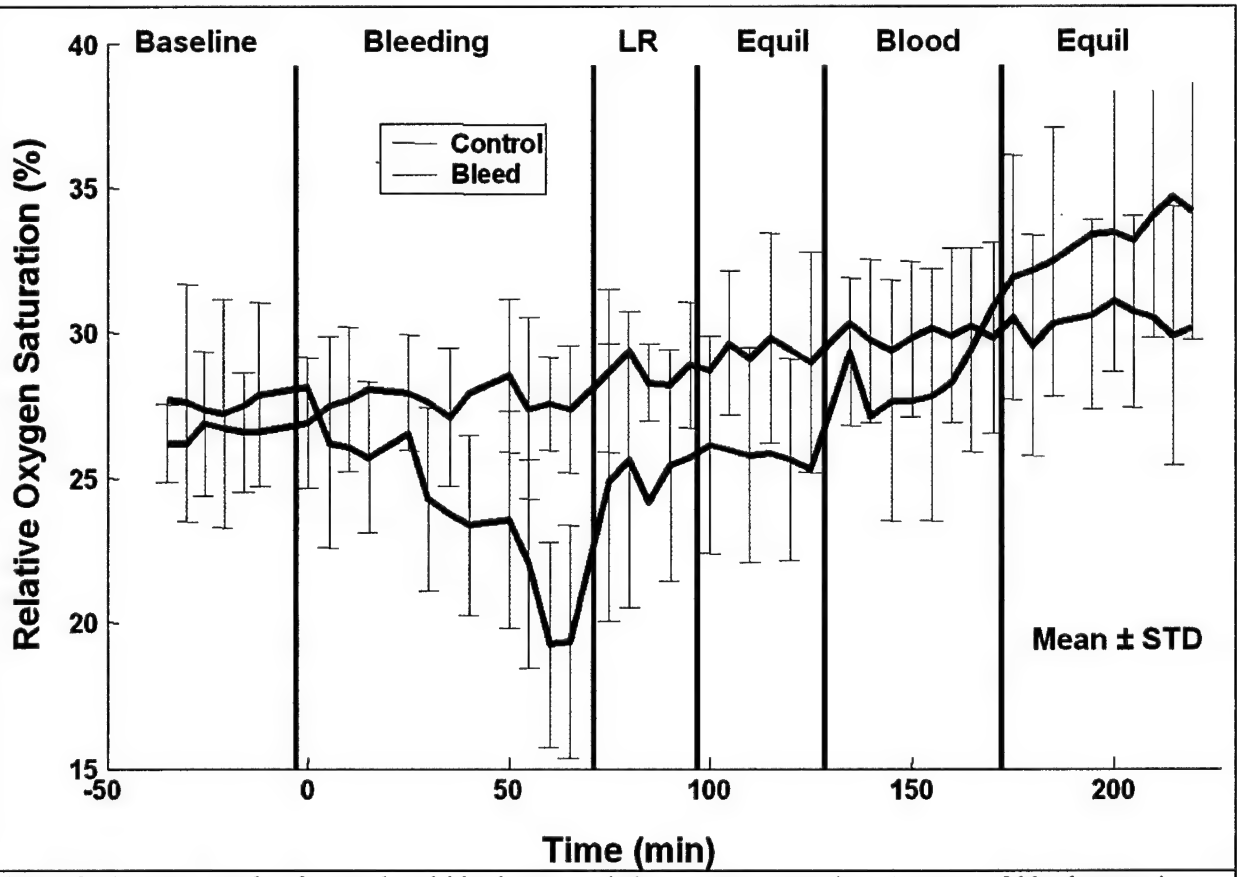

Figure 9: Average trends of control and bleed group relative oxygen saturation. Average of bleed group is shown in red; average of control group is shown in blue. Note approximately linear decrease in skin O_2Sat during entire bleed period and its partial recovery following LR resuscitation. Full recovery happens during blood reinfusion, resulting in a slight hyperemia. Error bars (one standard deviation) are shown on alternate timepoints to enhance visibility.

An easier-to-interpret version of the time courses of the mean grayscale O_2Sat values from the ROI on the hindlimb can be seen in Figure 9 (above). This graph shows the average value for each of the two groups (control, shown in blue, and bleed, shown in red), and the standard

deviations for each shown as error bars. The error bars are shown on alternate timepoints for the two groups to enhance visibility. There are no unusually large or small error bars not being shown. The very slight but not significantly different increase in O_2sat over time for the control animals can be clearly seen. During the bleed period, there is a consistent decrease in the group mean O_2Sat. Following LR resuscitation there is a rapid recovery to a higher oxygenation level, although not as high as for the control group. The O_2Sat remains stable during the equilibration phase and then increases again during blood resuscitation, overshooting the level seen in the control groups, perhaps an indication of hyperemia.

Total Hemoglobin Time Course Analysis

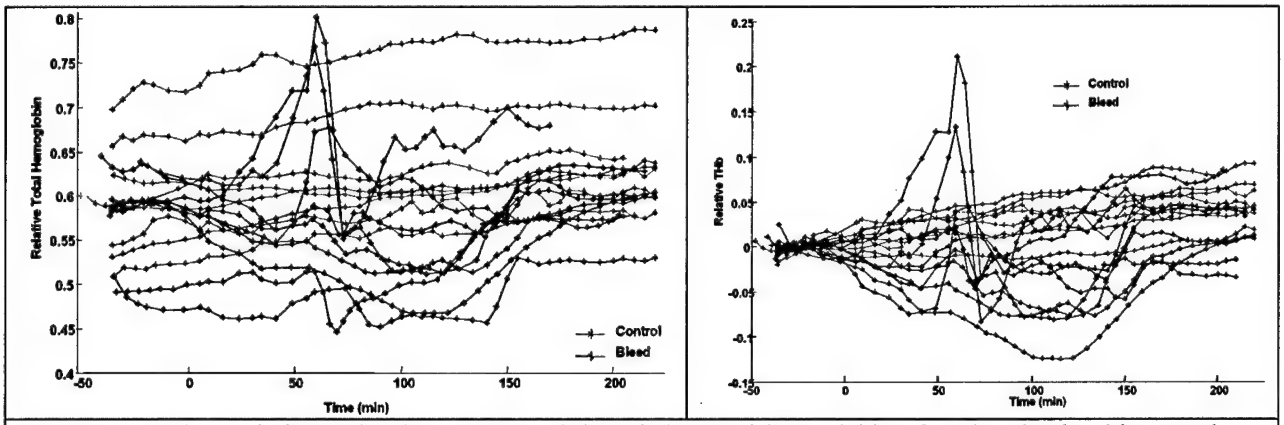

Figure 10: Left panel shows the time courses of the relative total hemoglobin of each animal, with control animals shown in green and bleed animals shown in red. Right panel shows the same data which has been baseline corrected by subtracting the mean of the baseline period (image cubes 1 through 6) from each time point. Key time points of interest: 0: begin bleed; 70: begin LR resuscitation; 120: begin blood resuscitation

Figure 10 (above) shows the trends over time of the total hemoglobin levels calculated for the 2" x 2" ROI from the hindlimb. The control animal's trends are shown in green and the bleed animal's trends are shown in red. There is a considerable variation in the starting THb levels among all animals, but there is no statistical difference between control and bleed animals during baseline (see left panel of Figure 10).

The right panel of Figure 10 shows the baseline subtracted THb trends, where the mean THb value for the baseline period (t = -50 to t = 0 min) is subtracted from the entire time course. It can be clearly seen that each of the bleed animals underwent a significant change in their THb levels during the course of the study while the control animals remained at a constant THb level (or a slightly increasing one). Most of the bleed animals showed a decrease in THb during the bleed period (t = 0 to t = 75 min), with a further decrease in THb during and following LR resuscitation, which is consistent with there being less total blood in the skin. The THb levels recovered to baseline (or very nearly to baseline) following blood resuscitation.

It can be clearly seen that a few of the bleed animals exhibited an unexpected and paradoxical **increase** in their THb levels during the bleed period. Closer inspection of the individual time courses shows that each bleed animal showed either a large increase in THb during bleed, or a small increase right at the end but before LR resuscitation. This was a completely unexpected

outcome, but is potentially useful in constructing an algorithm to predict survivability or adequacy of resuscitation.

Hypotheses:

a) Initial decrease in cardiac output and forward flow with hemorrhage in the absence of arteriolar vasoconstriction may cause increased pooling of blood in the skin and perhaps indicates less capacity for compensation in severe shock;
b) The changing hematocrit and blood volume in the skin during shock causes an increase in the pathlength of the light through the tissue, thus increasing the apparent amount of hemoglobin measured.

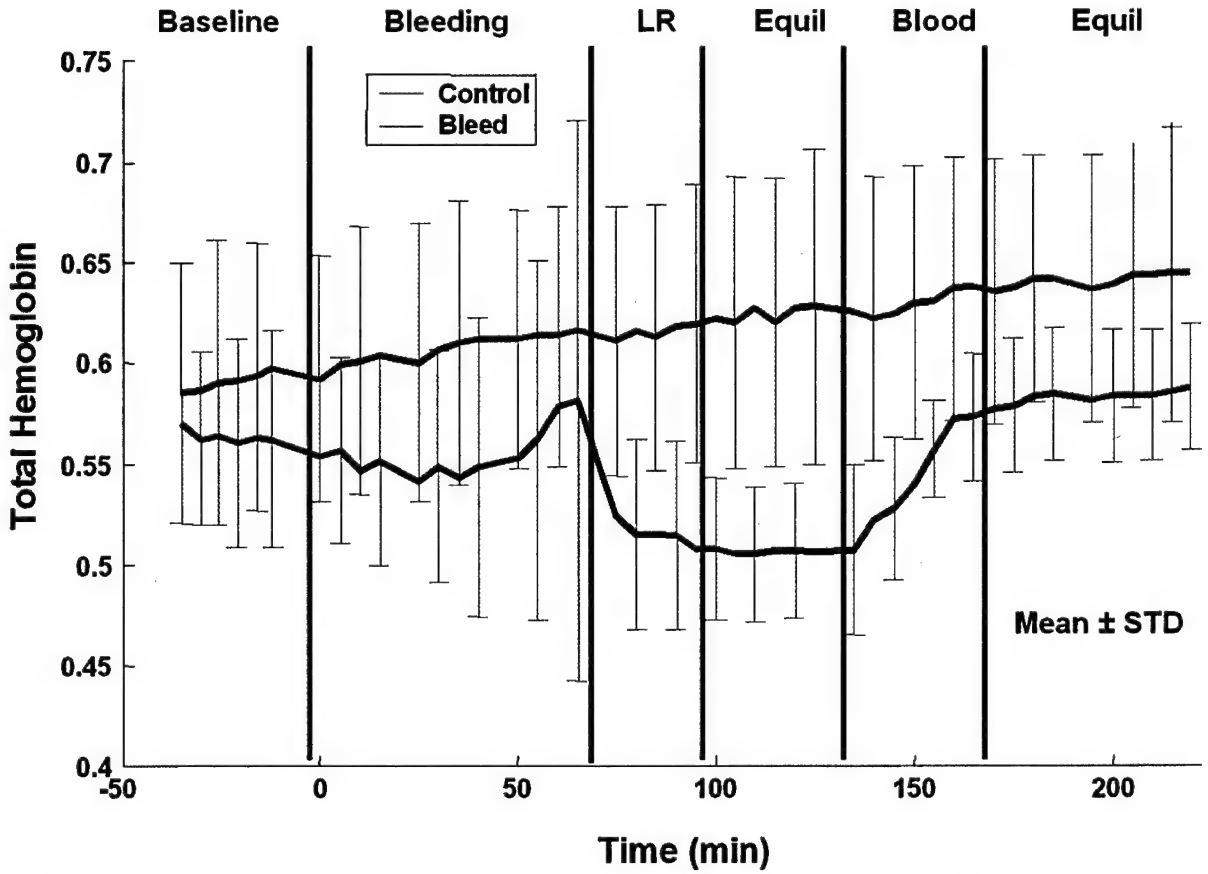

Figure 11: Average trends of relative total hemoglobin for control and bleed groups. Average of control animals is shown in blue; average of bleed animals is shown in red. Following LR resuscitation, the THb level of the bleed groups is significantly lower than the control animals, and then recovers almost to baseline following blood reinfusion. Error bars (one standard deviation) are shown on alternate timepoints for clarity.

The average time courses of the two groups (bleed, shown in red, and control, shown in blue) can be seen in Figure 11 (above). As with the O_2sat group averages, the control group appears to have a slow increase in THb during the study, although it is not statistically significantly different from beginning to end. The bleed group average begins to drop during the start of the bleed period, but then shows a slight increase towards the end of the bleed period. This is due to

the effects of the three animals that showed a marked increase in THb in this period (*cf.* Figure 10). Note also the increase in the standard deviation of the group in this period (t= 40 to t = 75 min).

Following LR resuscitation, there is a drastic decrease in the THb levels in the skin, which is consistent with the now greatly reduced hematocrit of the animals. The THb levels remained constant during the equilibration period following LR resuscitation and then as expected showed a nice linear increase during blood reperfusion (t = 130 to t= 170 min). The bleed group THb average then returned to approximately the level of the baseline period, although not quite as high as the control group became during the same time period.

Statistical Analyses

Overall Imaging Variable Analyses

In order to calculate a single p-value for the comparison between the bleed and control groups for the entire experiment, we require an overall descriptor for each imaging variable. The basic hypothesis of the hypovolemia study is that the HSI variables will be different between control and shock groups. To test this, we require an overall measure of the impact of shock on the HSI variables (*i.e.*, a single summary number per variable per animal). To do this we Simply using the mean is not powerful enough, nor does it account for the directionality of the data – *viz.*, the problem that the THb time courses of some of the animals decrease on bleed but increase for others. To avoid this issue, we used "pathlength" as a descriptor, and can be used for overall experimental p-value or for analysis at each time point. An equation for the pathlength of each time series can be seen in Equation 1 at right.

$$P = \sum_{i=1}^{n-1} \left| x_i - x_{i+1} \right|$$

Equation 1: Pathlength calculation[3]

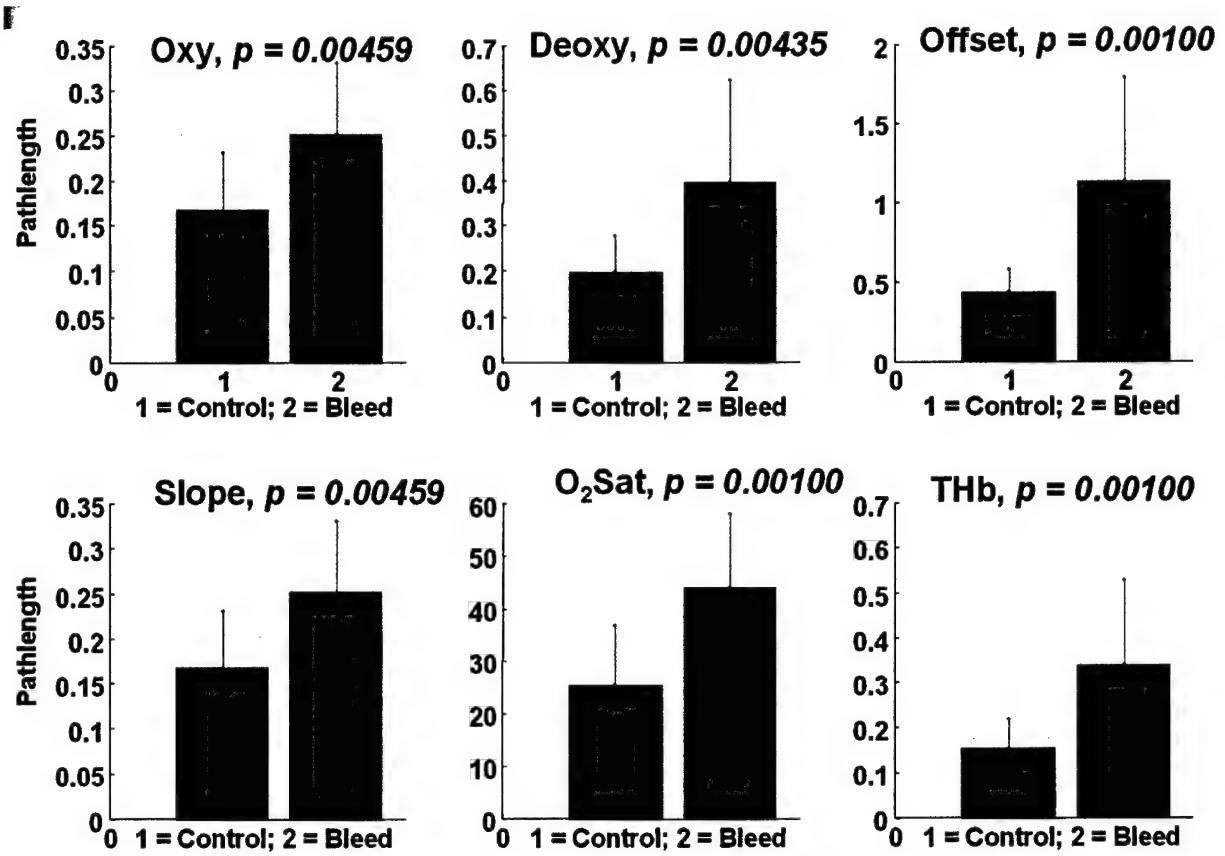

Figure 12: Shows the average (± one standard deviation) of the six imaging variables (oxy-Hb, deoxy-Hb, offset and slope coefficients and the O_2Sat and THb) for the bleed and control groups, with the control group on the left and the bleed group on the right. Also shows the results (p-value) for the t-tests on the pathlength calculations for each of the imaging variables.

There are six imaging variables: the four variables calculated directly from the HSI data (oxy-Hb, deoxy-Hb, offset and slop) and two variables calculated from the four (O2Sat and THb). O2Sat and THb were included in the results because of the immediate medical utility of these summary variables and the ease of interpretation of their results. The pathlength over the course of the study was calculated for each of these variables.

A two-sided t-test was performed on each of the six variables, dividing the data into two groups: bleed and control, the results of which can be seen above in Figure 11. For each variable, the bleed group had a statistically significantly larger pathlength than the control group. P-values for the six variables ranged from 0.004 to 0.001. The relative sizes and scatter of the distributions of the pathlengths of the six variables can also be seen in Figure 11.

Since the pathlength reflects an overall summary of the amount of change that happens during the course of the protocol, it is not surprising that the pathlength for the bleed group is larger on average than the pathlength for the control group for all six variables.

Summary of Hypovolemia Results

Using the HSIMM methodologies developed for this study, it was possible to clearly differentiate ($p << 0.01$) between control and bleed groups in a porcine hypovolemia model. A

stable hypovolemia model and data processing methods were developed to enable the transition of the technology and methodology into routine use at the Institute of Surgical Research. A pilot hypothermia study was performed, and HSIMM parameters were found to vary both with core temperature and skin contact temperature during hypothermia.

- Statistically significant difference in the magnitude of the pathlength between bleed and control groups for all six imaging variables
- Pathlength for all six imaging variables was longer for the bleed than for the control group, indicating that the hypovolemia caused larger changes in HSI variables relative to controls
- There was a significant decrease in O2Sat in bleed animals relative to control animals early during hypovolemia and that this decrease recovered on resuscitation.

Results from the Hypothermia Study

Five animals were used in the hypothermia study (plus 7 controls from the hypovolemia studies above). In order to understand the parameters and boundaries which best deliver data relative to the use of HSIMM in hypothermia, each animal underwent a slightly different set of cooling and warming protocols. The general protocol was as follows, with each animal's specific differences from the general protocol enumerated further below.

Each animal was prepared for the protocol identically to the hypovolemia animals (both control and bleed groups) so that the control animals for the hypovolemia study could be used as controls for the hypothermia study as well. This involved identical placement of arterial and venous lines and a splenectomy, as well as a stabilization period following preparation before beginning the baseline period of data collection.

Individual protocols

For all animals in the hypothermia study, there were two means of cooling and two means of warming used. For cooling, the temperature of the underblanket (which normally is used to keep the animal at a constant temperature during surgical procedures) was reduced to 4 C. This was done at approximate t = -10 min for all animals. At t = 0 min, ice packs were applied to the head, neck and thorax of the animal, and the entire upper torso of the animal shrouded with a space blanket (a thin blanket silvered on one side). For warming, the opposite pattern was followed. 10 min before the ice packs were removed, the temperature of the underblanket was set to 42 C (the warmest possible setting which would not burn the animal). Following that, the ice packs were removed and the upper torso of the animal was covered with a Bair Hugger set on full warm. See Appendix A for a complete description of methods.

The first animal's protocol was not accomplished consistently enough to allow its HSI results to be utilized for the general hypothermia results. However, despite not being able to utilize the imaging results, a great deal was learned about the methodologies and timings required, the understanding of which was used in the subsequent animal's protocols. The first animal was therefore considered to be a method development animal.

Overall Results

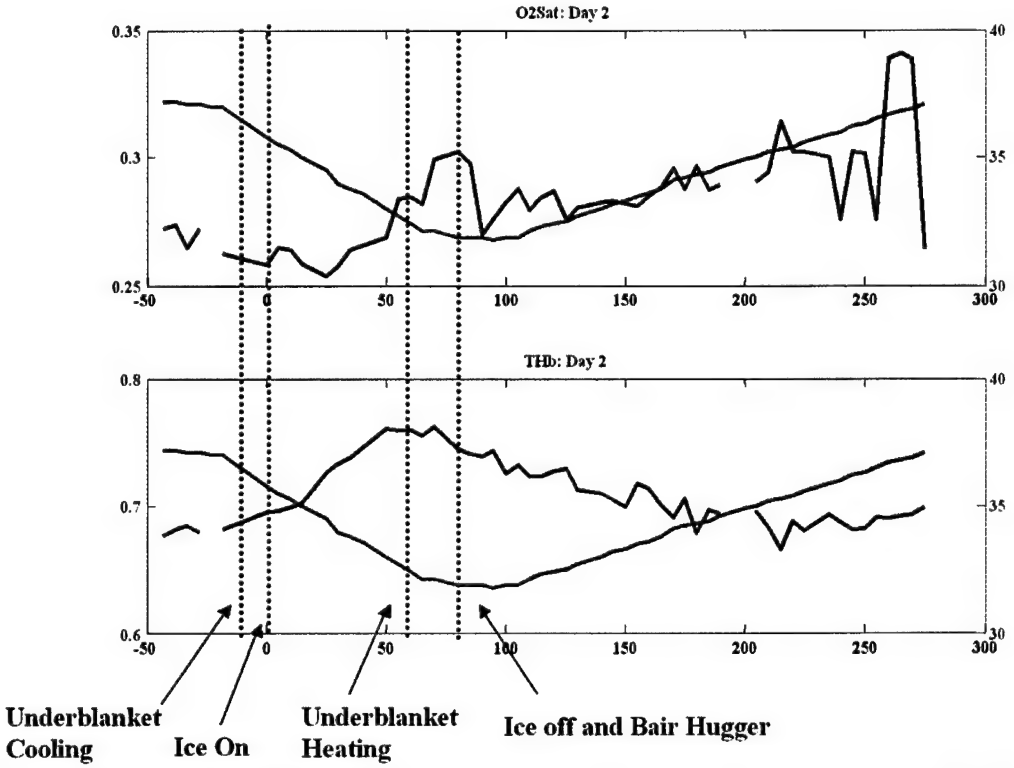

Figure 13: Second animal's hypothermia results. Rectal temperature is shown in green; O_2Sat (upper panel) and THb (lower panel) are shown in blue. Note that the THb trend changes when the under-blanket cooling parameters were changed, which is before the internal temperature of the animal begins to respond.

The upper panel of Figure 13 shows the trend over time of the O_2Sat of the skin of the inner hindlimb of animal two as well as showing the trend in rectal temperature during the course of cooling and warming. The rectal temperature, which began at 38 C, was lowered to 31 C, and rewarming was followed to 38 C. The skin THb begins to respond immediately to the change in the temperature of the underblanket of the animal (as is the case in all animals studied), unlike the rectal temperature, which showed a lag before responding to the underblanket temperature change. The temperature decrease in the animal is approximately linear until the warming begins at about 60 min. There is considerable inertia in the cooling of the animal, as can be seen in the overshoot of the rectal temperature, with actual core warming as recorded by rectal temperature occurring some 30 to 40 minutes after the physical surface warming began. Again, this is consistent among all animals and is consistent with our expectations from theoretical considerations and clinical experience..

The O_2Sat trends of animal two (upper panel, Figure 13) show a slight and slow increase during the course of the study. However, as all of the control animals showed either a stable O_2Sat or a slightly increasing O_2Sat during the course of the study (see hypovolemia section, above), and since there are no obvious changes in the rate or direction of change of the O_2Sat at the changes in the cooling and warming, there appears to be no significant impact of this degree of moderate hypothermia on measures of skin oxygenation and oxygen extraction .

The lower panel of Figure 13 shows the trend over time of the THb. Unlike the O_2Sat, the THb trends show clear indications of responding to the cooling/warming cycle. Immediately on changing the temperature (cooling) of the underblanket, the THb level in the skin begins to rise (t = -10 min). The rate of change of the THb increased slightly after the ice was put in place. Following that, the increase was approximately linear until the temperature of the underblanket was increased to 42 C. Immediately on changing the temperature of the underblanket, the THb level in the skin of the exposed thigh not exposed itself to surface warming began to decrease, even though the rectal temperature of the animal would not begin to respond for another 30 min. The decrease in THb in the skin proceeded approximately linearly until a baseline level was reached at *ca.* t = 220 min. As seen in a few cases within the hemorrhagic shock model, this again this may implicate that under certain circumstances, venous pooling in the skin may have a greater overall impact than arteriolar vasoconstriction, which would be associated with an overall decrease in THb.

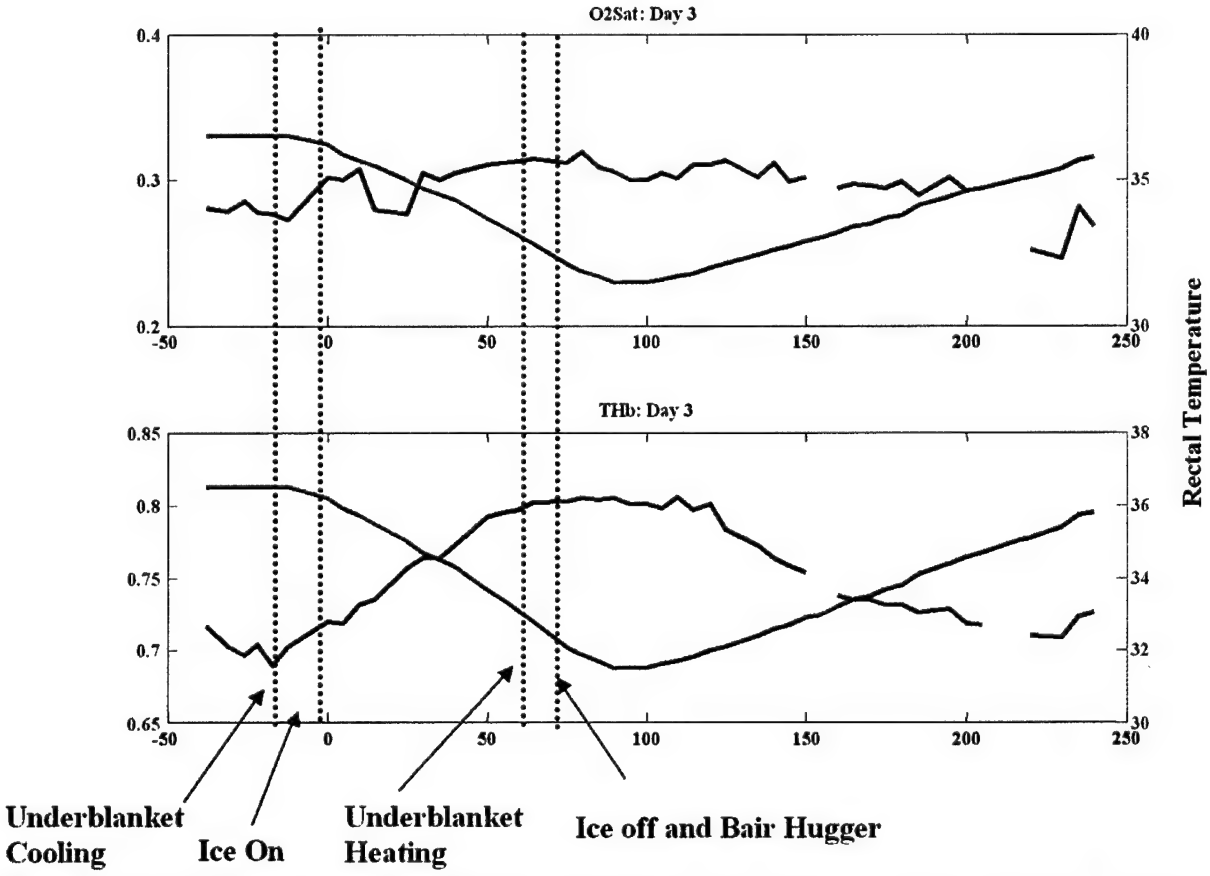

Figure 14: The third animal's hypothermia results. Rectal temperature is shown in green; O_2Sat and THb are shown in blue. Note that again the THb trend changes when the under-blanket cooling parameters were changed, which is before the internal temperature of the animal begins to respond while the O_2Sat values hardly change.

The third animal yielded results consistent with those of the second, as can be seen above in Figure 14. The rectal temperature of the animal began to decrease immediately with underblanket cooling, with considerable overshoot following the beginning of warming. The

O_2Sat trends were approximately constant during the course of the study, although this animal showed a slight but statistically insignificant decrease in O_2Sat following the onset of warming.

The THb trends of the animal are also consistent, with an immediate increase in THb seen on underblanket cooling, and immediate change in the rate of change of the THb trend immediately on underblanket warming. There was a slight overshoot in THb levels following onset of warming (t = 60 to t = ~90 min), but clearly the changes in THb rate of change are associated with warming. The THb then took approximately 120 min to return to its baseline level.

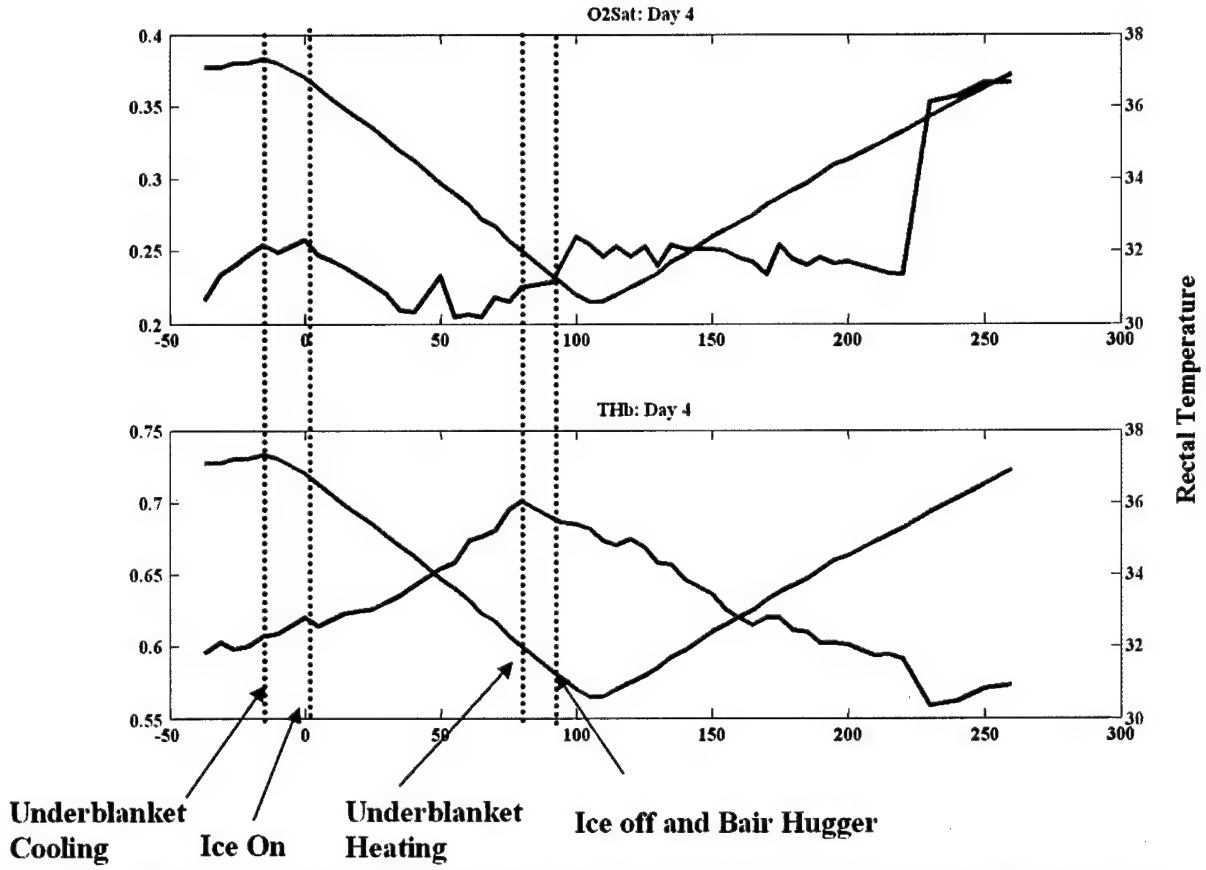

Figure 15: The fourth animal's hypothermia results. Rectal temperature is shown in green; O_2Sat and THb are shown in blue. Note that again the THb trend changes when the under-blanket cooling parameters were changed, which is before the internal temperature of the animal begins to respond while the O_2Sat values hardly change.

The fourth animal's results (Figure 15, above) are also consistent with the other animals'. The rectal temperature begins to respond immediately on underblanket cooling, and overshoots by approximately 30 min following the beginning of warming.

The O_2Sat trends of animal four again remained approximately constant during the study (see upper panel, Figure 15). The large jump in the O_2Sat at t = 230 min is an experimental artifact attributed to movement of the lighting system relative to the animal and should be disregarded.

The THb levels of this animal followed the same general pattern seen in the other animals: the THb levels began to rise immediately on decreasing the temperature of the underblanket and began to drop immediately on increasing the temperature of the underblanket. In this case, there was no time lag between the effects of the underblanket temperature on the THb levels.

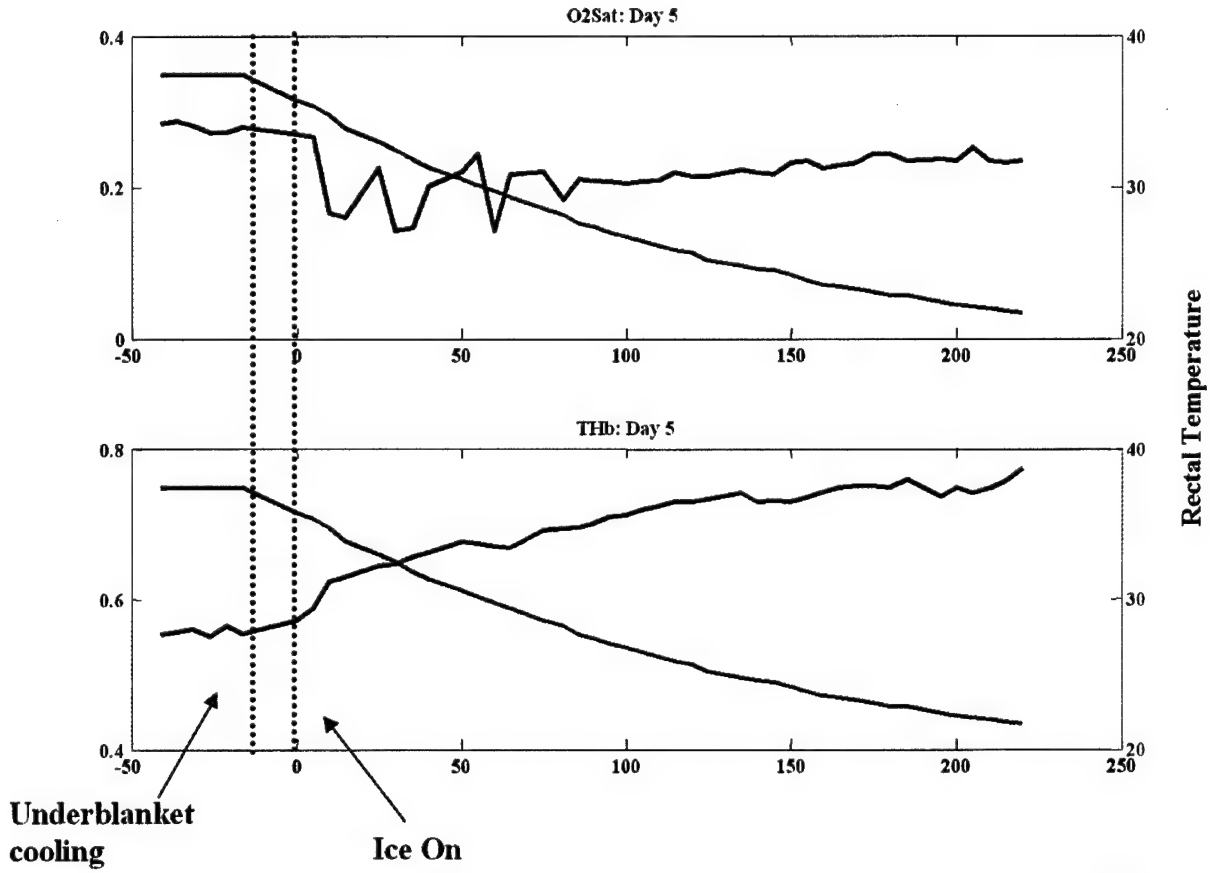

Figure 16: The fifth animal's hypothermia results. Rectal temperature is shown in green; O_2Sat and THb are shown in blue. Note that again the THb trend changes when the under-blanket cooling parameters were changed, which is before the internal temperature of the animal begins to respond while the O_2Sat values hardly change.

Because we had seen no real changes in the skin O_2Sat within the range of moderate hypothermia (down to 31 C rectal temperature) in the other animals, we decided to take the fifth animal down much farther (to 22 C rectal temperature) to look for possible changes during extreme cooling (see Figure 16, above). This animal was cooled continuously from t = 0 until the end of the study, and the rectal temperature (shown in green, Figure 16 above) shows a continuous decrease, although the rate of cooling decreased slightly over time.

The O_2Sat of the fifth animal also showed no significant changes over the course of the study. There was a drop in O_2Sat seen immediately after the application of ice packs (t = 0 min). However, this is attributed to an accidental moving of the animal in the field of view and does reflect an actual change in O_2Sat. For the rest of the study, the O_2Sat remained approximately constant, showing the slight increase over time seen in most of the control animals.

The THb level of the skin continued to increase throughout the cooling period (from t = -10 min to the end of the study). The rate of increase in the THb level approximately mirrors the rate of decrease in the rectal temperature of the animal (see lower panel, Figure 16, above).

Hypothermia Summary

The HSI results of the hypothermia portion of this study are intriguing. On one hand, as expected, there was a clear connection between hypothermia and HSIMM imaging parameters. On the other hand, the *a priori* expectation was that both the O_2Sat and THb levels in the skin would decrease as a result of the hypothermia (due to the reduced skin blood flow which is thought to occur during hypothermia), and this clearly was not the case.

For all animals, the O_2Sat level remained approximately constant during the entire protocol, which was identical to the pattern seen for the control animals. For all animals, the THb level in the skin **increased** during cooling and returned to a normal baseline level following rewarming. In addition, while in general changes in the THb level of the skin are approximately correlated to the rectal temperature, the causality seems to be more complicated. The THb level in the skin begins to change when the temperature of the underblanket is changed, even if the rectal temperature of the animal continues to change for some period of time after this. This would imply that the skin blood flow is also connected to external stimulus (warm/cold) applied to the skin and not solely to the core temperature of the animal

It is interesting to put this together in terms of generalized stasis, with venous pooling initially ahead of arteriolar vasoconstriction. The lack of change of O_2Sat measurements speaks to skin homeostasis throughout a range of temperatures and perhaps reflects a decrease in metabolic demand at lower temperatures. The rapidity of the THb response after the initiation of surface temperature manipulation but before impact on core temperature speaks to the possibility of a neurally-mediated control of skin perfusion and metabolic rate.

There are several other hypotheses for why the THb levels in the skin should increase on contact with a cooling surface and decrease on contact with a warming surface. One that is also consistent with what we saw in the hemorrhage protocol is that the relative THb level which is being calculated from the HSI data is being affected by changes in the pathlength of the photons in the skin, and that the pathlength of photons in the skin is being affected by the changes in perfusion caused by contact with warming and cooling objects. It has been hypothesized that the major cause of light scattering in the skin is from the platelets themselves, and a reduction in the number of platelets (amount of blood, or local hematocrit) would allow the penetration of photons much further into the skin than for normal levels of blood. This could account for the apparent increase in THb.

Given that the skin of each animal when hypothermic was pallid and appeared by eye to be almost translucent, one can assume that there was a reduced amount of blood in the skin (results not shown). If that is in fact the case, then the latter hypothesis above might explain the inverted relationship between THb and hypothermia. Future experiments will need to be designed to test out which (if either) of these hypotheses are correct.

Key Research Accomplishments

- Refined and validated HSIMM image acquisition and data processing techniques, optimizing them for use in shock models. Given the spatial size and distribution of the heterogeneities related to vascular supply and reactivity seen in lower limbs (in this study) and on the under side of the chin (in previous studies), it was concluded that imaging an area of approximately 2.5 x 5 inches would be optimal.
- Developed a robust, repeatable and stable porcine model for hemorrhagic shock which could now be applied to performing quantitative determinations of survivability or of the effects of specific treatment regimens or resuscitation protocols.
- Developed a set of requirements for a robust porcine model for hypothermia and a series of hypotheses to test regarding the measurement of skin physiology and metabolism using HSI.
- Performed a 17 animal study using a hemorrhagic shock model to determine whether HSI could be used non-invasively and without contact to determine whether an animal was in shock and to define the specific HSIMM characteristics most useful in making this determination. This study was a clear success: numerous imaging parameters were clearly differentiable between bleed and control groups.
- Obtained clearly demonstrable and statistically relevant differences between control and bleed groups in a porcine hypovolemic shock model using HSIMM methodologies
- Defined separate HSIMM patterns (diffuse homogeneity, "feathering", mottling) within the pigs subjected to hemorrhage that may be useful in determining survivability or adequacy of resuscitation.
- Developed protocols for software for interfacing the HSIMM data collection into the standard LabVIEW acquisition scheme at the Institute of Surgical Research, clearing the way for easier integration of HSI methods into ongoing protocols there.
- Transitioned to the Army a tested research-grade HSIMM system.
- Determined data processing and experimental design parameters for transitioning HSIMM technologies into human model and clinical studies of shock.

Reportable Outcomes

Presentations

1. Federation of Analytical Chemistry and Spectroscopy Societies (FACSS) Presentation
Cancio, L.; Batchinsky, A.; Lewis, E.N.; Freeman, J.; Lew, R.A.; Mansfield, J.R.* "Non-Invasive Determination of Hypovolemic Shock Using Hyperspectral Imaging" Presented at the Federation of Analytical Chemistry and Spectroscopy Societies (FACSS) Annual Meeting, Ft. Lauderdale, FL, October, 2003.

Abstract:

Hyperspectral imaging (HSI) has been shown to be useful in monitoring several medical conditions, which to date have generally involved local changes in skin oxygenation in isolated regions of interest such as skin flaps or small burns. Here, by contrast, we present a study in which HSI was used to assess the cutaneous manifestations of significant systemic events. Visible HSI of the ventral surface of the leg was used to monitor changes in skin

oxygenation during hypovolemic shock induced by hemorrhage in a porcine model, and to monitor the subsequent recovery following resuscitation. Changes were seen both quantitatively, in the levels of skin oxygenation and total hemoglobin, and qualitatively, in the observed spatial distribution of perfusion-related changes in the skin. Seventeen animals were studied (8 shock and 9 controls), with significant differences seen between groups.

2. Institute for Surgical Research Presentation

Cancio, L.; Batchinsky, A.; Lewis, E.N.; Freeman, J.; Lew, R.A.; Mansfield, J.R.* "The Use of Hyperspectral Imaging for Combat Casualty Care" Presented at the U.S. Army Institute of Surgical Research Scientific Seminar, August, 2003.

3. SPIE presentation

Leopoldo C. Cancio, Derek Brand, Jeffrey Kerby, Jenny E. Freeman, Michael Hopmeier, James R. Mansfield "Visible Hyperspectral Imaging: Monitoring The Systemic Effects of Shock and Resuscitation" Presented at Photonics West, BiOS, International Society for Optical Engineering, San Jose, CA, 2002

Abstract:

Hyperspectral (HS) imaging has been useful in the monitoring of several medical conditions, which to date have generally involved changes in skin oxygenation in isolated regions of interest such as skin flaps or small burns. Here, by contrast, we present a study in which HSI was used to assess the cutaneous manifestations of significant systemic events. HS imaging of the ventral surface of the lower jaw was used to monitor changes in skin oxygenation during hypovolemic shock induced by pulmonary contusion and hemorrhage in a porcine model, and to monitor the subsequent recovery of oxygenation following resuscitation. Changes are seen both quantitatively, in the level of skin oxygenation as determined by the fitting of reference hemoglobin and deoxyhemoglobin spectra to sample spectra, and qualitatively, in the observed spatial distribution or pattern of oxygenation-related changes in the skin. Linear regression was used to correlate these changes with invasively obtained parameters to include mixed venous oxygen saturation and systemic arterial blood pressure. Historically, the assessment of skin color and mottling has been an important, albeit inexact, component of resuscitation algorithms. Now, it is possible to analyze these variables during shock and resuscitation in an objective manner. The clinical utility of these advances needs to be determined.

Publications

1. Journal of Biomedical Optics (in preparation)

Leopoldo C. Cancio, Jenny E. Freeman, Andriy Batchinsky, Robert A. Lew, E. Neil Lewis, James R. Mansfield "Methodology for hyperspectral imaging based monitoring during shock", manuscript in preparation.

2. Journal of Trauma (in preparation)

Leopoldo C. Cancio, Jenny E. Freeman, Andriy Batchinsky, Robert A. Lew, E. Neil Lewis, James R. Mansfield "Using skin oxygenation and total hemoglobin images to monitor hypovolemic shock", manuscript in preparation.

3. Diabetes Technology & Therapeutics (Invited Paper)

Robert Gillies, Jenny E. Freeman, Leopoldo C. Cancio, Derek Brand, Michael Hopmeier, James R. Mansfield "Systemic Effects of Shock and Resuscitation Monitored by Visible Hyperspectral Imaging" Diabetes Technology & Therapeutics, an invited paper in a special issue on Military Metabolic Monitoring, Volume 5, Number 5, 2003, 847 – 855.

Abstract:

Background: Hyperspectral imaging (HSI) has been useful in monitoring several medical conditions, which to date have generally involved local changes in skin oxygenation of isolated regions of interest such as skin flaps or small burns. Here, by contrast, we present a study in which HSI was used to assess the local cutaneous manifestations of significant systemic events.

Methods: HSI of the ventral surface of the lower jaw was used to monitor changes in skin oxygenation during hypovolemic shock induced by hemorrhage with additional pulmonary contusion injury in a porcine model, and to monitor the subsequent recovery of oxygenation with resuscitation.

Results: Quantitative and qualitative changes were observed in the level of skin oxygenation during shock and recovery. Quantitative values were obtained by fitting reference spectra of oxyhemoglobin and deoxyhemoglobin to sample spectra. Qualitative changes included changes in the observed spatial distribution or pattern of skin oxygenation. A mottled pattern of oxygen saturation was observed during hemorrhagic shock, but not observed during hypovolemic shock or following resuscitation.

Conclusions: Historically, the assessment of skin color and mottling has been an important, albeit inexact, component of resuscitation algorithms. Now, it is possible to analyze these variables during shock and resuscitation in an objective manner. The clinical utility of these advances needs to be determined.

New Projects and Other Outcomes

1. **Began shock/Hypovolemia/oxygen diagnostics database**

In order to develop a usable field unit for a HSIMM device, we have begun documenting the range of responses, both in terms of mean grayscale changes in HSIMM parameters and in terms of the spatial heterogeneity of these parameters, for a large number of humans and animals.

2. **Three new TMM projects applied for**

As a result of the success of this project, both scientifically and in terms of the collaboration between ISR and HyperMed, three new TMM grants have been applied for (FY2003) and a two more applications are in preparation (FY2004).

3. **SBIR application (January)**

Building on the foundation of this project, as well as other related projects, further hardware and software modification of this technology will be addressed in an SBIR proposal to be submitted in in January.

4. **Collaboration on NIH grant with Dr. Aristides Veves**

Our proven ability to utilize HSI as a means of interrogating systemic disease has opened an avenue for collaborative research with Dr. Aristedes Veves of the Beth Israel Deaconess Medical Center in Boston, MA, working on the early detection of feet at risk of developing foot ulcers. A successful collaborative effort resulted in an NIH-funded project looking at comparing HSI, laser

Doppler imaging and MRI-based phosphate imaging for the effects of iontorphoresis on diabetic feet.

Conclusions

The purpose of this study was to begin to explore the possibility of using HSIMM as a tool for the assessment of shock and resuscitation in the research laboratory, the clinical environment and the battlefield. We have previously demonstrated the capabilities of HSI to deliver information about local tissue that can predict its viability over time. It was our intent here to see if it was possible to develop a system that had the capability to interrogate the skin and instead pf providing data about only local tissue viability, could deliver information about the systemic physiology and potentially the viability of the entire organism. As the primary outcome of this study, we believe that we have built a HSIMM system and have proven its capabilities to assess systemic physiology by interrogating local tissue.

We believe that we have refined our HSI system and methodology sufficiently and have demonstrated the capacity of this system and these methods to provide sufficiently sensitive and specific data to warrant further studies into the applicability for HSIMM to assess shock and resuscitation and hypothermia and that it can provide information otherwise unobtainable or in advance of extant techniques.

We have been clearly able to correlate HSIMM information with the shock state and have defined several groups of imaging patterns within the shocked animals which may deliver information as to their underlying metabolic state, appropriateness of resuscitation or survivability. We believe that we have demonstrated that the HSIMM system has capabilities that warrant support of further animal work based on the models that we have established to explore its capabilities to predict outcome or to direct therapy. We also believe that having clearly demonstrated the capabilities of our HSIMM system in the porcine model, expansion into human studies of shock and monitoring are warranted. Additional work with resuscitation under hypothermic conditions is also intriguing and we now have the capabilities to approach questions relative to therapeutic interventions and outcomes with our system and methods. While not necessary for HSIMM to provide well correlated and clinically useful data, from a theoretical standpoint, additional experiments to query the THb and O_2Sat results, possibly by comparing visible and NIR readings of THb and O_2Sat under similar circumstances would be of theoretical interest in terms of understanding more of the physiologic fundamentals reported in our imaging results.

In summary, we believe that HSI has the real potential to be a useful research and clinical tool for the assessment of systemic physiology and pathology. By creating the HSIMM system and refining standard research methodology under this study protocol, we have clearly made advances toward the delivery of a useful device.

Appendices

A. Porcine Hypovolemic Shock Model Methods

Animals

This study was approved by the Institutional Animal Care and Use Committee. All animals were cared for in accordance with the guidelines set forth by the Animal Welfare Act and other federal statutes and regulations relating to studies involving animals, and by the 1996 *Guide for the Care and Use of Laboratory Animals* of the National Research Council. All animals were maintained in a facility approved by the Association for the Assessment and Accreditation of Laboratory Animal Care, International. Seventeen (9 in the hemorrhage and 8 in the control group) female Yorkshire pigs weighing 36.4 $\pm$ 0.11 kg were used. The animals were quarantined for one week and were fasted overnight prior to the experiment.

Surgical Preparation

Animals were premedicated with 250 mg IM Telazol (Lederle Parenterals, Inc. Carolina, PR). After induction of anesthesia with isoflurane delivered through a mask they were intubated, and were placed on a Datex-Ohmeda ventilator with a tidal volume of 10ml/kg and a respiratory rate of 12/min. The rate was adjusted to achieve normocapnea ($PaCO_2$ = 35-45 mm Hg). Anesthesia was maintained with a mixture of isoflurane (2-2.5%) and room air. Percutaneous sheath introducers (8.5 Fr; Arrow International, Inc. Reading, PA) were inserted into the carotid artery and external jugular vein bilaterally, and a 10F Foley catheter was inserted into the urinary bladder. A splenectomy was performed via a midline laparotomy. The splenic artery was tied off before splenectomy to allow drainage of blood from the spleen into the circulation. An infusion of lactated Ringers solution (LR) at 1.5 times the spleen weight was administered immediately after the splenectomy. At the end of surgery the isoflurane was decreased to 0.6% and an infusion of ketamine (250-350 ug/kg/min) was begun. The ketamine-isoflurane anesthesia was continued until the end of the study. Depth of anesthesia assessment and anesthetic dose adjustments were made as needed. Core temperature was maintained between 37-39° C by means of an external heating pad (Gayman Industries, Inc., NY, NY).

A Swan-Ganz catheter (VIP Oximetry 782HF75, Edwards Life Sciences, Irvine, CA) was inserted via the external jugular vein introducer sheath to permit measurement of the pulmonary arterial pressure (PAP), central venous pressure (CVP), thermodilution cardiac output (CO), pulmonary arterial wedge pressure (PAWP), mixed venous saturation of oxygen (SVO_2), mixed venous blood gases, and core temperature. One of the carotid arterial introducer sheaths was used for measurement of the arterial blood pressure (ABP). Clinical pressure transducers (Transpac IV trifurcated monitoring kit, Abbott Critical Care Systems, Abbott Laboratories, North Chicago, IL) were used. The heart rate was obtained from the electrocardiogram. All physiologic waveforms were digitized and were acquired at a rate of 500 Hz to a personal computer running custom LabVIEW data acquisition software (National Instruments Corp., Austin, TX).
Regional skin temperature was monitored on both hindlimbs using the Physiotemp BAT -10, Type T Thermocouple Thermometer system (Physiotemp Instruments INC, Clifton NJ). All values digitally recorded into the data acquisition system.

Initially, measurements of cutaneous (lower extremity) sympathetic nerve activity were attempted via placement of microneurographic electrodes in the lumbar sympathetic nerve. However, this proved technically challenging and was later abandoned in order to focus on the main objectives of the proposal.

Experiment: Hemorrhage and Resuscitation

After a stabilization period (1-2 hours) baseline data were collected. The animals in the hemorrhage group then underwent withdrawal of blood through the carotid line with a syringe. Three withdrawals, each 10ml/kg, were performed at a constant rate of 1ml/kg/min. Blood was collected into a bag containing CPDA (J-520 blood collection unit, Jorgensen Laboratories, Loveland, CO). Each of the three 10-min hemorrhage periods was followed by a 15-min observation period. Following the third observation period, the animals were resuscitated with LR at 1.5 times the shed blood volume. (Those animals who developed preterminal hemodynamic instability during the third observation period, manifested by decreasing heart rate and profound hypotension, received LR resuscitation sooner.) The duration of the LR resuscitation period was 25 min. Additional fluid to exceed the initial resuscitation volume was then administered as needed to return the heart rate and blood pressure towards baseline values. The 25-min LR infusion period was followed by a 30-min observation period. This was followed by a 25-minute period during which the shed blood was reinfused. The animals were observed for an additional hour thereafter and then were euthanized. Blood and LR were infused using a fluid warmer (Ranger blood/fluid warming system, Model # 254, Augustine Medical, Prairie, MN). Animals in the control group underwent similar surgical preparation and received a maintenance LR infusion at 100 ml/hour.

Data were obtained at the following time points: baseline, after each 10ml/kg blood withdrawal, after LR resuscitation, and after blood reinfusion.

Experiment: Hypothermia

In a pilot study, an additional 5 animals weighing 36.2 ± 0.45 kg were used. These subjects underwent analogous preparation/surgery as those in the hemorrhage group. From the starting core temperature the animals were continuously cooled down over 1hour and 40 minutes by placing the animal on a cooling blanket (Gayman Med Therm II Model MTA 5942 Hyper/Hypothermia System, Gaymar Industries, Inc., NY) set at 4 deg C , lowering the room temperature to 65 deg F and covering the head, neck, armpits, and torso with plastic bags filled with ice, covered on top with another cooling blanket set to 4 degrees C.

The target cooling point was 31 degrees C. The duration of cooling mimicked the duration of the 3 consecutive bleed-equilibration sessions described for the main protocol.

Our goal was to avoid dropping the core temperature below the 31degree target point. To achieve this after reaching 33 degrees the blanket and room temperature were set at 42 deg. C and 86 deg F respectively. The animal continued in cooling reaching 31 degrees and started warming up shortly after that. Rewarming was carried out until baseline core temperature values were reached.

Body temperature was monitored via: Pulmonary artery catheter and rectal temperature probe. Regional skin temperature was monitored on both hindlimbs using the Physiotemp BAT -10,

Type T Thermocouple Thermometer system (Physiotemp Instruments INC, Clifton NJ). All values digitally recorded into the data acquisition system.

Assays

Arterial and mixed venous blood samples were collected into pre-heparinized 1-ml disposable syringes at each sampling time point. They were analyzed using an AVL Omni Modular System (Roche Diagnostics GmbH Graz, Austria).

Arterial blood was collected at each time point and was certrifuged. Plasma samples were stored at -70° C until analysis. Plasma catecholamines (epinephrine, norepinephrine, and dopamine) were measured by radioimmunoassay (TriCat ™ RIA, Immunobiological Laboratories, Hamburg, Germany). Assays were performed by KMI Diagnostics Laboratory Services (Minneapolis, MN). Briefly the samples were extracted. The extracted material was acylated in the presence of ^{125} I epinephrine and antiserum, followed by precipitation with a second antiserum. The precipitate was separated from the solution by centrifugation and aspiration. The tubes with the precipitate were counted by gamma-counting. Sample values were determined by interpolation from a standard curve.

B. Laser Doppler Imaging Methods

A Laser Doppler Perfusion Imager (Periscan PIM II, Perimed AB, Stockholm, Sweden) was used at each time point to obtain images based on non-contact laser Doppler flowmetry of the region of interest. Mean perfusion was calculated off line for 16 by 16 pixel windows within in the ROI.

C. Hyperspectral Imaging Methods

Camera System

Imaging data were collected using a 10-bit Kodak Megapixel 1.6*i* CCD camera (Roper Scientific, Trenton, NJ) fitted with an AF 50 mm *f*/2.8 EX Macro camera lens (Sigma Corporation, Tokyo, Japan). Wavelength selection was provided by a VIS2 visible wavelength liquid crystal tunable filter (LCTF) (Cambridge Research & Instrumentation, Woburn, MA) with a nominal 7 nm bandpass, which was fitted to the front of the camera lens.

Data Collection

Images were collected as 256 x 382 pixel arrays by binning in 4x4 squares in software using a custom software interface developed in LabVIEW (National Instruments, Austin, TX). Images of the inner hindlimb and a white reflectance standard were collected at 5 nm intervals from 500 to 600 nm with the integration times being adjusted such that the brightest image in each sequence filled approximately 80% of the full well capacity of the CCD. Five images at each wavelength were added together. The data resulting from each of these sequences is known as an image cube, each of which requires approximately 2 min to acquire.

HSI data processing

The image cubes were then converted to optical density units by ratioing the sample data to data acquired from a white background using a standard Beer's Law algorithm. A complete description of this methodology can be found elsewhere.[4] A four-term linear regression fitting of oxy-hemoglobin, deoxy-hemoglobin, offset and slope terms was then be performed on each of

the spectra in the image cube. Reference human oxy and deoxy hemoglobin spectra were obtained in electronic format.[5] The regression fit coefficients were be used to calculate a relative oxygen saturation percentage and total hemoglobin value for each spectrum in the image cube.[6] All spectral computations were done using Matlab (The Mathworks, Natick, MA).

D. Statistical Analysis

Outline of Statistical Analysis Plan for Comparison of Imaging and Physiological Variables

The major question is to distinguish the two types of animal (shock and control). The outcome measure for these analyses was therefore the binary factor 'type'. Note, subsequent reports will focus on the secondary endpoints of heart rate (hrate) and arterial blood pressure (abp). The independent variables that predict the endpoint (dependent variable) were divided into two sets; image variables and metabolic variables.

Imaging: oxy-Hb, deoxy-Hb, offset, slope, O2Sat and THb

Metabolic: central venous pressure (CVP); systolic pulmonary arterial pressure (PAP_S); diastolic pulmonary arterial pressure (PAP_D); mean pulmonary arterial pressure (PAP_M); exhaled CO2 (CO2); systolic arterial blood pressure (ABP_S); diastolic arterial blood pressure ABP_D); mean arterial blood pressure (ABP_M); pulmonary artery wedge pressure (PAWP); rectal temperature (RECTEMP); right skin temperature (TEMP1); left skin temperature (TEMP2); arterial blood temperature (BLODTEMP); and heart rate (HRATE).

The data were gathered over time or in stages:

- Stage 1 was baseline.
- Stages 2 and 3 were the first bleed and first recovery.
- Stages 4 and 5 were the second bleed and second recovery.
- Stages 6 and 7 were the third bleed and third recovery.

A summary of the timing, stages and events of the protocol can be found in Table 1, above.

Results for Univariate Statistical Models

There were no differences between any imaging or physiological variables between shock and control groups during the baseline phase ($p > 0.1$). During the bleed and recovery phases, very early separators of shock from control groups were metabolic variables: ABP_M and PAP_M were significant in stage 2 (Bleed One). Later separators include imaging variables: Oxy-Hb and Slope were significant at stage 5 (Recovery Two). Deoxy-Hb values never separated enough to significantly ($p < 0.05$) distinguish control from shock groups.

Multivariate Discrimination Between Bleed and Control Groups

Various multivariate models that discriminated between bleed and control groups were studied. Models were constructed for early and for late stages using logistic regression to predict the binary endpoint "type" with two categories "shock" and 'control".

Results for Early Stages

ABP was the best single discriminator and did so in stages 2 and 3(first bleed and recovery). A model that includes ABP and TEMP1 slightly increased discrimination. Adding more variables to the model did not significantly increase discrimination. More precisely,

For stages 2 and 3 (1st bleed and recovery) the 'best' model was "Model: shock = abp".

To evaluate how well this model predicted we looked at the estimated probability of "shock" for each animal. The predictive equation obtained from the logistic regression model that produces a predicted probability between zero and one. If that probability exceeds 0.5 then we say that the model predicted 'shock'. Otherwise, we say that 'the model predicted 'no shock' or 'control'.

Recall that each animal was measured several times with each stage. Thus, the actual endpoint was animal-time. We compared actual type and predicted type. As shown in Table 2, 30+29 = 59 animal-times were predicted correctly and 6+3 = 9 incorrectly. In other words, 59/68 = 87% were predicted correctly and 13% were predicted incorrectly.

Therefore, Percentage correct (agreement) is 87%.

Table 2		Actual Shock		
		Yes	No	Total
Predicted Shock	Yes	30	3	33
	No	6	29	35
	Total	36	32	

The model could be refined by adding another factor; namely, temp1, "Model shock = abp temp1". Again using predicted probability, discrimination improved with 93% predicted correctly and 7% incorrectly -- 93% agreement.

Results for Later Stages in Terms of Imaging Variables

Logistic regression models were constructed using only imaging variables. The 'best" early stage model for stages 2-3 was "Model: Shock = oxy deoxy", but this model only predicted 70% correctly. While no absolute standards exist, useful models should have correct prediction rates well over 50%. Hence, we looked at prediction at later stages.

At stages 2-3-4, 3-4, 3-4-5, 4-5, 4-5-6, 5-6, 5-6-7, and 6-7, the pair of variables, 'oxy deoxy', did better as the set of predictors than other combinations image variables. The best stages for prediction of shock with this pair of variables were stages 5-6 (2nd recovery and 3rd bleed) -- 88.9% predictions correct and stages 4-5 (2nd bleed and recovery) -- 85% predictions correct.

Each sequences of stages corresponds to a different dataset. An indication of a stable prediction formula is as the datasets vary there is little variation in the coefficients in the logistic regression models used to construct the prediction formulas. Table 3 presents the coefficients for eight series of stages; that is, eight different datasets. Models based on data from stages 2 and 3 differ form models based on later stages. This is reflected in the percentage of agreement that approaches 90% in stages 5-6.

The general conclusion is that the metabolic or physiological factors discriminate early on in the shock progression and that imaging variables discriminate later on in the process.

Table 3-Coefficients in Logistic Regression Models

Stages	Intercept	Oxy-Hb	Deoxy-Hb	Agreement
4-5	17.7	-61.5	-20.2	85%
4-5-6	15.9	-60.0	-16.6	86%
5-6	15.9	-63.7	-15.7	88.9
5-6-7	12.6	-58.5	-9.9	86.8%
6-7	10.6	-55.4	-6.5	87%
2-3	10.4	-25.2	-15.0	69%
2-3-4	11.6	-31.9	-15.6	71%
2-3-4-5-6-7	11.6	-43.4	-11.9	78%

- Statistically significant difference in the magnitude of the pathlength between bleed and control groups for all six imaging variables
- Pathlength for all six imaging variables was longer for the bleed than for the control group, indicating that the hypovolemia caused larger changes in HSI variables relative to controls
- There was a significant decrease in O2Sat in bleed animals relative to control animals during hypovolemia and that this decrease recovered on resuscitation.

Statistical analyses

Statistical analyses were done using SAS (Version 8, SAS Institute Inc., Cary, NC).

Mean Values by Stage for All Animals and Separately for Each Type

Primary Endpoints and Imaging Parametersfor Stages 2-7

Stage	hrate	abp	oxy	deoxy	osat	thb	offset	slope
ALL ANIMALS								
bl1*	95.01	76.21	0.15	0.43	25.96	0.59	1.43	0.15
rec1	100.47	71.25	0.15	0.44	25.58	0.59	1.41	0.15
bl2	107.35	70.50	0.15	0.44	25.08	0.59	1.39	0.15
rec2	116.44	68.90	0.14	0.45	23.89	0.59	1.39	0.14
bl3	119.80	65.26	0.14	0.46	23.61	0.60	1.39	0.14
rec3	135.37	63.00	0.13	0.47	22.23	0.61	1.43	0.13

Stage	hrate	abp	oxy	deoxy	osat	thb	offset	slope
CONTROL ANIMALS								
bl1	96.68	83.37	0.15	0.45	25.52	0.61	1.45	0.15
rec1	96.45	83.51	0.16	0.45	26.16	0.61	1.45	0.16
bl2	95.73	85.55	0.16	0.45	26.00	0.61	1.44	0.16
rec2	95.32	85.23	0.16	0.46	25.74	0.62	1.44	0.16
bl3	94.43	86.51	0.16	0.46	26.14	0.62	1.44	0.16
rec3	93.61	85.76	0.16	0.46	25.77	0.62	1.44	0.16

Stage	hrate	abp	oxy	deoxy	osat	thb	offset	slope
SHOCK ANIMALS								
bl1	93.52	69.84	0.15	0.42	26.34	0.57	1.41	0.15
rec1	104.04	60.34	0.14	0.42	25.07	0.56	1.38	0.14
bl2	117.69	56.34	0.13	0.42	24.22	0.56	1.33	0.13
rec2	135.22	54.38	0.12	0.43	22.25	0.56	1.35	0.12
bl3	143.67	45.25	0.12	0.45	21.07	0.57	1.34	0.12
rec3	174.67	41.57	0.11	0.48	18.69	0.59	1.43	0.10

* bl1 or bleed1 is stage2, rec1 or recovery1 is stage3,
bl2 or bleed2 is stage4, rec2 or recovery2 is stage5,
bl3 or bleed3 is stage6, rec3 or recovery3 is stage7.

Mean Values by Stage for All Animals and Separately for Each Type

Metabolic-Physiological Parameters for Stages 2-7

Stage	cvp	pap_S	pap_d	pap	co2	abp_s	abp_d	temp1	temp2	rtemp	bltemp
ALL ANIMALS											
bl1	4.25	20.10	9.87	14.92	3.42	90.42	63.88	34.45	34.50	36.14	37.02
rec1	3.95	19.18	9.50	13.94	3.42	86.14	59.99	34.41	34.62	36.17	37.06
bl2	3.30	19.54	9.40	14.06	3.01	84.69	59.74	34.48	34.71	36.19	37.08
rec2	2.98	17.75	8.43	12.87	2.99	82.84	58.68	35.07	35.39	36.22	37.13
bl3	3.16	18.27	8.88	13.24	2.74	80.04	54.65	35.06	35.35	36.22	37.07
rec3	3.17	19.40	8.35	13.49	2.69	78.23	52.45	35.01	35.35	36.27	37.24

Stage	cvp	pap_S	pap_d	pap	co2	abp_s	abp_d	temp1	temp2	rtemp	bltemp
CONTROL ANIMALS											
bl1	4.21	21.75	10.35	16.33	3.69	96.99	69.23	34.34	34.22	37.38	37.22
rec1	4.03	21.05	10.23	15.85	3.69	97.08	69.50	34.37	34.23	37.40	37.25
bl2	4.03	22.09	10.29	16.42	3.55	98.84	71.68	34.60	34.51	37.43	37.24
rec2	3.72	21.35	9.89	15.86	3.54	98.51	71.66	35.97	35.99	37.44	37.29
bl3	4.12	21.99	10.99	16.74	3.45	100.99	72.10	35.96	35.93	37.47	37.29
rec3	3.99	21.60	10.25	16.09	3.45	98.85	72.25	35.99	35.94	37.49	37.33

Stage	cvp	pap_S	pap_d	pap	co2	abp_s	abp_d	temp1	temp2	rtemp	bltemp
SHOCK ANIMALS											
bl1	4.30	18.64	9.42	13.68	3.17	84.59	59.12	34.54	34.74	35.04	36.84
rec1	3.89	17.51	8.77	12.25	3.17	76.41	51.53	34.46	34.96	35.07	36.89
bl2	2.69	16.99	8.38	11.69	2.53	71.37	48.51	34.37	34.89	35.10	36.94
rec2	2.40	14.37	6.87	10.07	2.50	68.91	47.15	34.27	34.86	35.14	36.99
bl3	2.25	14.77	6.63	9.96	2.08	60.33	38.23	34.22	34.80	35.04	36.86
rec3	2.39	17.33	6.45	11.05	1.97	58.82	33.82	34.09	34.80	35.13	37.15

References

1 Mansfield, J.R.; Sowa, M.G.; Mantsch, H.H. "Near Infrared Spectroscopic Reflectance Imaging: Methods for Functional Imaging and In-Vivo Monitoring" Proc SPIE. 3597, 222-233 1999.

2 Leopoldo C. Cancio, Derek Brand, Jeffrey Kerby, Jenny E. Freeman, Michael Hopmeier, James R. Mansfield "Visible Hyperspectral Imaging: Monitoring The Systemic Effects of Shock and Resuscitation" Proc. SPIE, Vol. 4614, 159-168.

3 KV Mardia Statistics of Directional Data, Chapter 8. Academic Press, London, 1972.

4 Mansfield, J.R.; Sowa, M.G.; Scarth, G.B.; Mantsch, H.H. "The Use of Fuzzy C-Means Clustering in the Analysis of Spectroscopic Imaging Data" Analytical Chemistry, 1997, 69, 3370-3374.

5 Prall S. Available online at: http://omlc.ogi.edu/spectra/hemoglobin/index.html

6 Robert Gillies, Jenny E. Freeman, Leopoldo C. Cancio, Derek Brand, Michael Hopmeier, James R. Mansfield "Systemic Effects of Shock and Resuscitation Monitored by Visible Hyperspectral Imaging" Diabetes Technology & Therapeutics, Volume 5, Number 5, 2003, 847-855.